Biochemical characterizations of a RelE/ParE superfamily toxin in Vibrio parahaemolyticus

张, 晶

https://doi.org/10.15017/1866256

出版情報：九州大学, 2017, 博士（システム生命科学）, 課程博士
バージョン：
権利関係：

Biochemical characterizations of a RelE/ParE superfamily toxin in *Vibrio parahaemolyticus*

2017

ZHANG JING

（张 晶）

Contents

Abbreviations

A_{280}	:	absorbance at 280 nm
Amp	:	ampicillin
ATP	:	adenosine triphosphate
bp	:	base pair
BSA	:	bovine serum albumin
cDNA	:	complementary DNA
CFU	:	colony forming unit
CFX	:	ciprofloxacin
DAPI	:	4', 6-dianidino-2-phenylindole
DNA	:	deoxyribonucleic adic
DTT	:	dithiothreitol
EDTA	:	ethylenediaminetetraacetic acid
Gyr	:	DNA gyrase
GyrA	:	A subunit of DNA gyrase
GyrB	:	B subunit of DNA gyrase
IPTG	:	isopropyl-β-D-thiogalactopyranoside
kbp	:	kilo base pairs
kDa	:	kilo dalton
LB	:	Luria-Bertani
OD	:	optical density
ORF	:	open reading frame
PCR	:	polymerase chain reaction
PDB	:	protein data bank
PFGE	:	pulsed-field gel electrophoresis
PSK	:	post-segregation killing
RNA	:	ribonucleic acid
RNase	:	ribonuclease
rpm	:	rounds per minute
SDS-PAGE	:	sodium dodecyl sulfate-polyacrylamide gel electrophoresis
SI	:	superintegron
TA	:	toxin/antitoxin
TAE	:	Tris-acetate-EDTA buffer
TBE	:	Tris-borate-EDTA buffer
TE	:	10 mM Tris-HCl, pH 8.0, containing 1 mM EDTA
Tris-HCl	:	Tris (hydroxymethyl) aminomethane hydrochloric acid
UV	:	ultra violet
V/cm	:	voltage/centimeter
VBNC	:	viable but nonculturable
β-ME	:	β-mercaptoethanol

Chapter 1

General introduction

1-1. Toxin-antitoxin (TA) systems

Toxin-antitoxin (TA) systems are composed of a toxin, which causes growth arrest by interfering with a vital cellular process, and a cognate antitoxin, which neutralizes the toxin activity during normal growth conditions (Page et al., 2016). TA systems were initially discovered, more than 30 years ago, as a plasmid-borne factor of post-segregational killing (PSK) (Ogura 1983; Gerdes et al., 1986b). Namely, the products of the toxin genes selectively kill the plasmid-free cells in the population, so as to promote plasmid maintenance in the daughter cells (Fig. 1-1). The selective activation of a toxin in cells that lost the TA-encoding plasmid is based on the instability of an antitoxin (Aakre, 2015). In the well-known TA systems, the antitoxins are more unstable than their toxins, and as a result the antitoxins must be continually transcribed in order for providing enough antitoxins to neutralize the toxins. For example, the first discovered TA system *ccdA-ccdB* was located in a mini-F plasmid. The antitoxin CcdA is more unstable than its toxin CcdB, and as a result *ccdA* must be continually transcribed in order to produce enough CcdA to neutralize CcdB. Cells that lose the mini-F plasmid can no longer produce CcdA, and the more stable CcdB is then freed to kill the plasmid-free cells (Van Melderen et al., 1994). This is applicable to another plasmid-born TA system *hok-sok*, only that the selectivity is based on RNA stability. Under normal station, the antitoxin *sok* produce an unstable antisense RNA to inhibit the translation of the toxin gene *hok*. Loss of the plasmid R1 triggers a rapid degradation of *sok* RNA, thus frees the production of the Hok toxin, leading to the killing of the plasmid-free cells (Thisted et al., 1992).

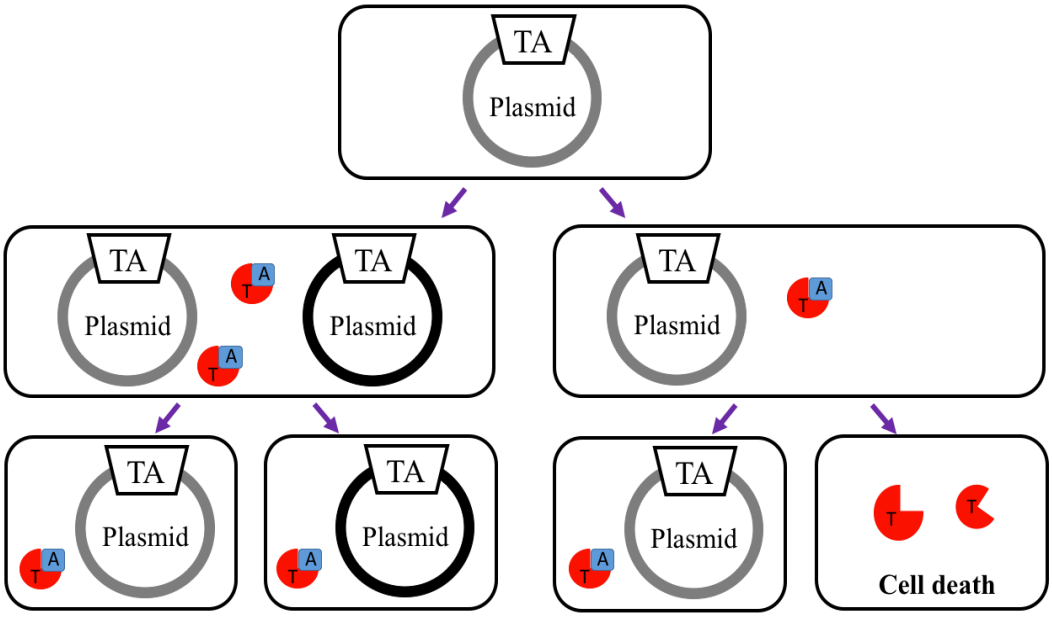

Fig. 1-1. Schematic representation of post-segregational killing (PSK) by plasmid-borne TA systems.

When a plasmid is correctly replicated and divided in the cells, an antitoxin forms a complex with a toxin to block its toxicity. If the plasmid fails to be given to the progeny, the antitoxin is selectively degraded by proteases, and then the activated toxin kills the cell. TA, T and A indicate toxin-antitoxin genes, toxin and antitoxin, respectively.

Shortly after the discovery of TA systems on plasmids, their identification on chromosomes was reported (Gerdes et al., 1986a). Since then, thousands of TA operons have been discovered not only in plasmids, but also on the chromosomes of most free-living bacteria (Aizenman et al.,1996; Masuda et al., 1993). Of all these TA systems, toxins are proteins, while antitoxins are either RNAs or proteins. The TA systems are so far classified into six classes, based on the mechanisms by which the antitoxins block the toxicity of their toxins (Fig.1-2). In the well- known type II TA systems, antitoxin and toxin mRNAs are synthesized from the same promoter and translated into proteins (Fig. 1-3). An antitoxin immediately forms a stable complex with a toxin to block its function. The antitoxin-toxin complex and the antitoxin also bind to the promoter to inhibit the expression of toxin-antitoxin genes. Under conditions of environmental stress, such as amino acid and carbon source limitation, labile antitoxins are selectively

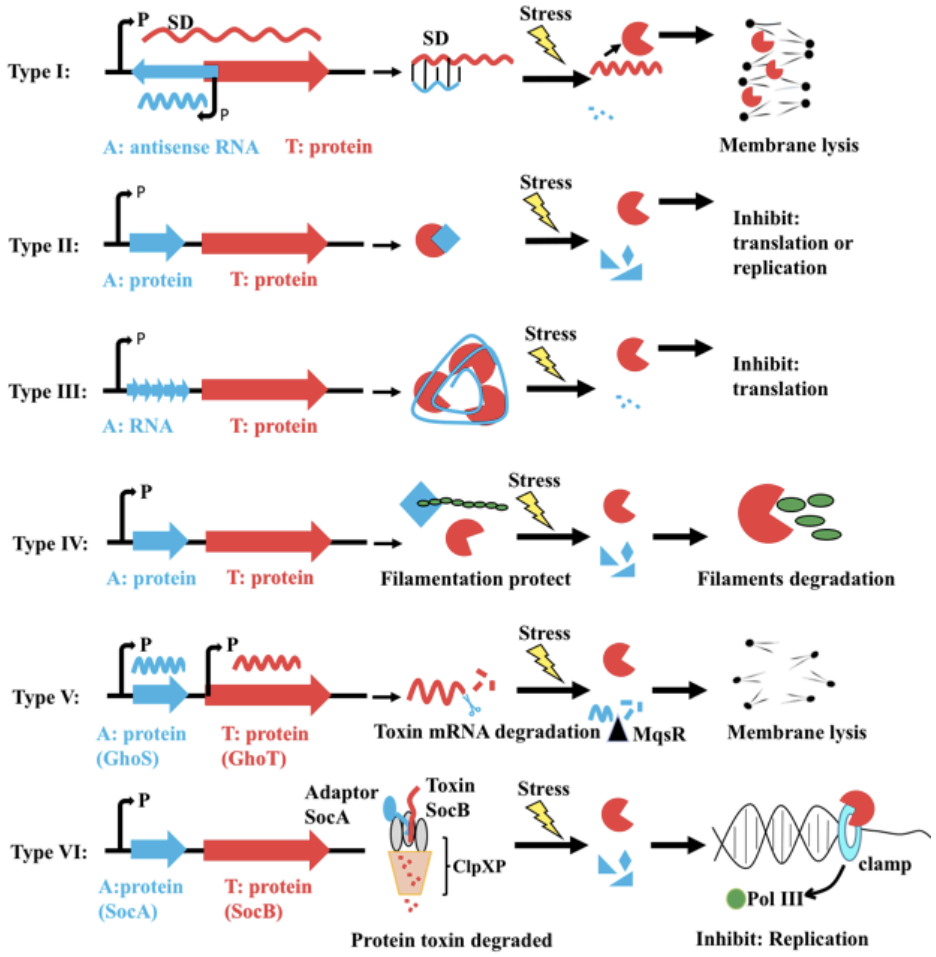

Fig. 1-2. Toxin-antitoxin (TA) systems.

Toxins are shown in red and antitoxins in blue. Type I: the sRNA antitoxin base pairs with toxin mRNA to inhibit translation; when activated by stress, the toxins function to destroy the cell membrane and disrupt ATP synthesis. Type II, both antitoxin and toxin are proteins; under growth conditions, the toxin is bound by the antitoxin, which inhibits its toxicity. Both the antitoxin and, in most cases, the TA complex bind the TA promoter to repress transcription. Under stress conditions, cellular proteases such as Lon and ClpXP are activated that preferentially cleave the antitoxins, freeing the toxins to inhibit growth by inhibiting translation or replication. Type III: the antitoxin sRNA is processed by the endoribonuclease (RNase) toxin, resulting in the formation of RNA pseudoknot-toxin complexes, which inhibit toxin activity. Type IV: the protein antitoxin stabilizes bacterial filaments, while the protein toxin disrupted them; in the absence of the antitoxin, this toxin-mediated defilamentation inhibits cell division. Type V: the antitoxin GhoS is an RNase specifically cleave the toxin ghoT mRNA; under conditions of stress, the mRNA of the antitoxin GhoS is degraded. This figure was cited from the ref. reported by Page et al (Page et al., 2016).

degraded by ATP-dependent proteases such as Lon, ClpXP, or ClpAP, leading to rapid growth arrest and cell death due to the cellular effects of toxins (Christensen et al., 2004; Fineran et al., 2009). The type II toxins inhibit cell growth by interfering with vital cellular functions, including DNA replication, protein synthesis, cell-wall biosynthesis and ATP synthesis (Short et al., 2013; Masuda et al., 2012).

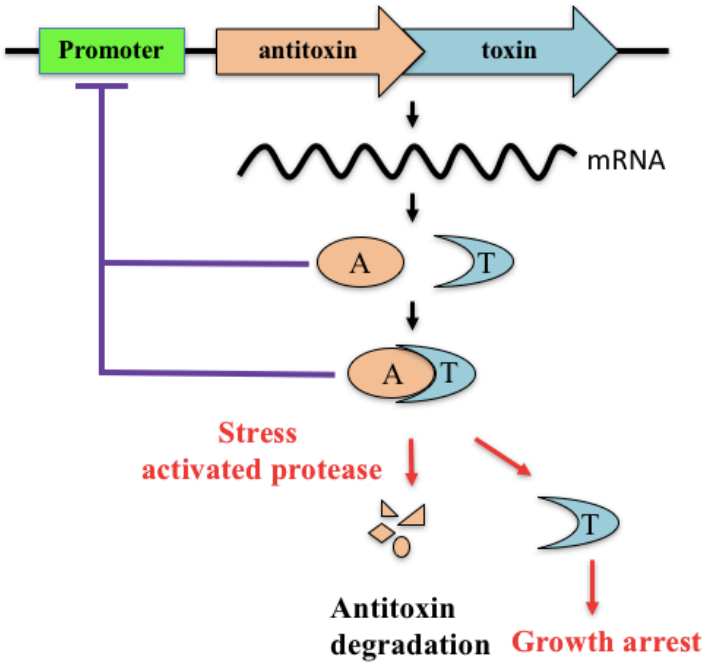

Fig. 1-3. Schematic representation of an operon encoding a type II toxin and antitoxin.

Antitoxin and toxin mRNAs are synthesized from the same promoter and both are translated into proteins. An antitoxin immediately forms a stable complex with a toxin to block its function. Under stress conditions, the antitoxin is degraded so that the toxin is activated, resulting in growth arrest.

Recent findings suggest that chromosomally encoded copies of toxins and antitoxins function as metabolic stress response elements to manage their metabolism to cope with different sources of stress. That is, chromosomally encoded TA systems have been suggested to be a genetic element involved in induction into dormancy, such as a viable but non-culturable state (VBNC) or persistence, but their biological functions are still

under debate (Wang et al., 2012; Aakre et al., 2013; Christensen et al., 2001; Wang et al., 2013).

1-2. *Vibrio parahaemolyticus* and a viable but non-culturable (VBNC) state

Vibrio parahaemolyticus is a Gram-negative, halophilic asporogenous rod that is straight or has a single, rigid curve. It was first discovered by Fujino et al. following the large outbreak of food borne disease in Japan, which caused 272 illnesses and 20 deaths in 1950s (Fujino et al., 1953). Since then, it has been recognized as the leading causal agent of human gastroenteritis associated with seafood consumption all over the world (Letchumanan et al., 2014). *V. parahaemolyticus* grows in the presence of 0.5 ~ 8% NaCl (optimum 3 ~ 6%) at 10 ~ 42°C (optimum is 35 ~ 37°C). It is also tolerant to a pH range of 5.6 ~ 9.6 (optimum is 7.6 ~ 8.0). Notably, the organism has an extremely short generation time (8 ~ 12 min) than *Escherichia coli* (25 ~ 30 min), under appropriate conditions (3% NaCl, 37°C). *V. parahaemolyticus* is able to exist in multiple cell types according to a variable circumstance (Fig. 1-4). It can either be a swimmer cell in liquid cultures or a swarmer cell in highly viscous environments (McCarter, 1999).

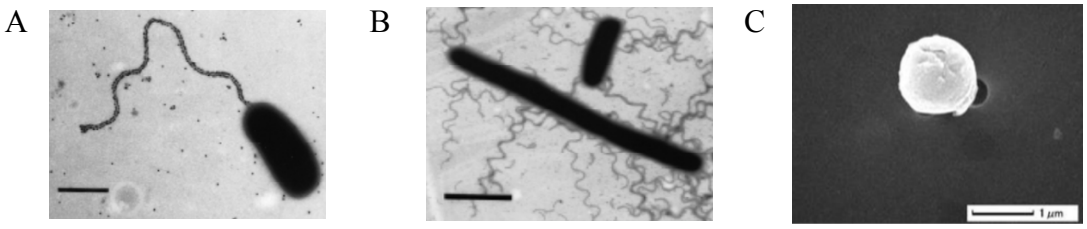

Fig. 1-4. Viable identities of Vibrio parahaemolyticus.

(A) Electron micrograph of a swimmer cell (McCarter,1999); (B) Electron micrograph of a swammer cell (McCarter,1999); (C) scanning electron micrographs of a cell entered into the VBNC state (Hino et al., 2014).

Genome sequencing of *V. parahaemolyticus* RIMD2210633, one of the pandemic strains (Kanagawa phenomenon positive, serotype O3:K6), showed that it contains two circular chromosomes (Chromosome I and II). The larger chromosome I consists of 3,288,558 bp, encoding for 3,079 proteins and the chromosome II is 1,877,212 bp, producing 1,752 proteins. When compared the *V. parahaemolyticus* genome sequence with that of *V. cholerae*, another diarrhoea-causing Vibrio with two circular chromosomes, a super-integron (SI) was identified on the chromosome I in *V. parahaemolyticus* (Makino et al., 2003). SI is a large gene-capture and excision system found on chromosome II in *V. cholera*, and it is characterized by a site-specific integrase gene closely associated with a cognate recombination site attI and a promoter Pc followed by a large array of gene cassettes (Rowe-Magnus et al., 2001). In addition, a large number of the genes located in SI have unknown functions (Mashimo, 2006). The SI in *V. parahaemolyticus* (48 kb) contains 78 ORFs, as shown in Fig. 1-6, while that in *V. cholerae* (126 kb) includes 179 genes, and their gene organization and sequence are perfectly distinct from each other. Nevertheless, it is known that SIs are highly conserved during evolution of each species, and however, the molecular basis of the conservation remains unclear.

Another characteristic feature of *V. parahaemolyticus* is that it can even enter into the viable but non-culturable (VBNC) state to escape harsh environmental conditions such as temperature and salinities downshift, nutrient starvation. (Bates and Oliver., 2004; Wong and Wang., 2004; Hino et al., 2014). The VBNC state is a unique state distinct from death. Cells in VBNC state are still alive and possess a lot of physiological function as a viable cell. Yet, they have no ability to develop into colonies on suitable media as viable cell. When the cell exists in a VBNC state, the cellular morphology, cell wall, membrane composition, physical and chemical resistance, gene expression, adhesion properties, virulence potential and metabolism are different to those of the viable cells (Li et al., 2014). The resuscitation property of the VBNC state can regain its virulence under suitable conditions (Du et al., 2007). This characteristic of VBNC cells is responsible for latency and recurrence of diseases (Pai et al., 2000; Rivers and Steck., 2001). Therefore, it is of great importance to illuminate the mechanisms of

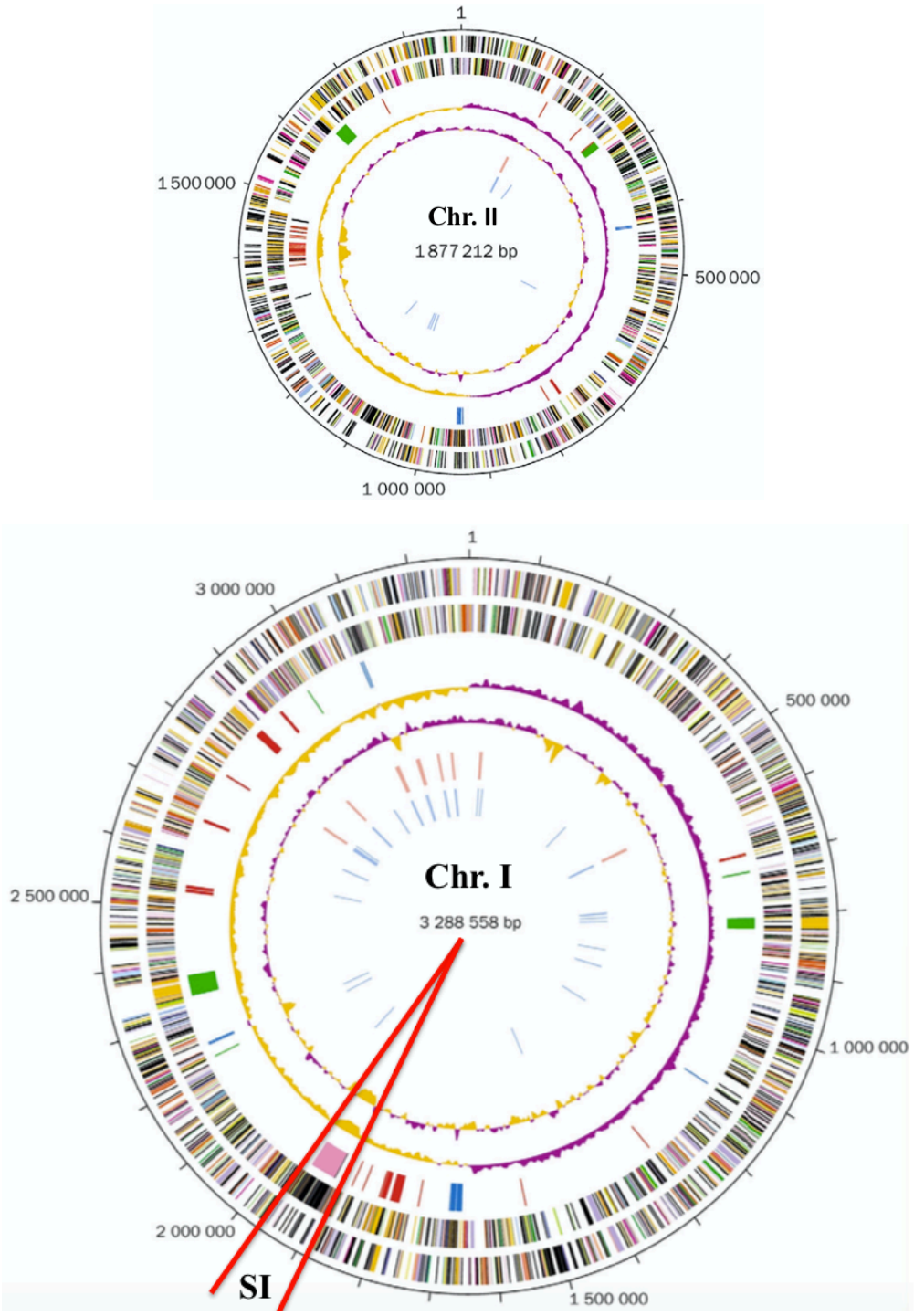

Fig. 1-5. The two chromosomes in *V. parahaemolyticus.*

V. parahaemolyticus contains two circular chromosomes. The larger chromosome I is 3,288,558 bp and the chromosome II is 1,877,212 bp. This figure was cited from the ref. reported by Makino et al. (Makino et al., 2003). SI stands for super-integron. The organization of SI is depicted in Fig. 1-6.

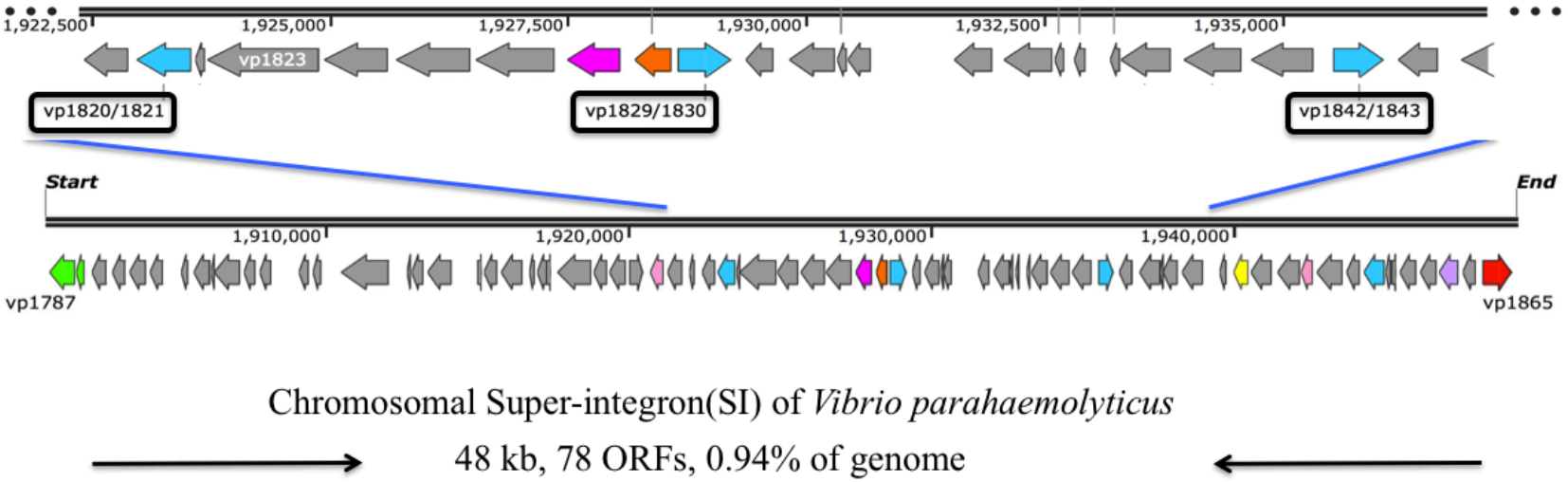

Fig. 1-6. Gene organization in the super-integron (SI) in the *V. parahaemolyticus* chromosome I.

Organization of genes in the SI. Color in green, red, gray, blue, light purple, pink, yellow, orange and magenta stand for transposase, Vp intIA, hypothesis protein, toxin-antitoxin gene, threonine efflux protein, a protein involved in cell-cycle regulation, acetyltransferase, PnuC protein, spermine/spermidine acetyltransferase BltD individually. This was created by SnapGene (http://www.snapgene.com).

induction into the VBNC state to effectively prevent bacterial infections and cure infected patients.

Since Colwell and coworkers first reported on the VBNC state (Xu et al., 1982), this phenomenon has now been described for over 50 bacterial species using various criteria for viability and discussed in relation to dormancy and persistency (Oliver et al., 2010). Although the VBNC state has been believed to be a survival strategy in response to certain harsh environmental stresses, no specific factors have been identified because many environmental conditions induce the VBNC state in different bacterial species. Recently, there is a growing evidence that activation of TA systems is one of the mechanisms known to trigger such a state with low metabolic activity (Hayes et al., 2009).

1-3. TA systems discovered in *V. parahaemolyticus*

In a previous study (Hino et al., 2014), we found three gene clusters, *vp1821/vp1820*, *vp1829/vp1830* and *vp1842/vp1843*, in the *V. parahaemolyticus* genome database have sequence homology to those encoding the *E. coli* type II TA proteins, YefM/YoeB, DinJ/YafQ and DinJ/YafQ, respectively. Expression of the putative toxin gene, *vp1820* or *vp1843*, in *E. coli* strongly inhibited cell growth, while co-production of the putative antitoxin gene, *vp1821* or *vp1842*, neutralized this effect. In contrast, the expression of *vp1830* in the presence of 0.2% arabinose had no influence on cell growth. These results suggested that *vp1842/vp1843* serve as a TA system in *V. parahaemolyticus*. It was further found that although Vp1820 has protein synthesis inhibitory activity, Vp1843, unlike the *E. coli* homologue YafQ, has neither protein synthesis inhibitory activity nor ribonuclease activity. Rather, the expression of *vp1843* in *E. coli* resulted in a morphological change in the cells, while co-expression with *vp1842* had no influence on the cell shape.

During the course of the previous study, we found that Vp1843 has sequence homology not only to *E. coli* YafQ, but also to *Caulobacter crescentus* ParE (Fig. 1-7) (Dalton and Crosson., 2010). Phylogenetic studies have found that YafQ and ParE belong to the RelE/ParE superfamily (Fig. 1-8), folding into a similar fold, despite the

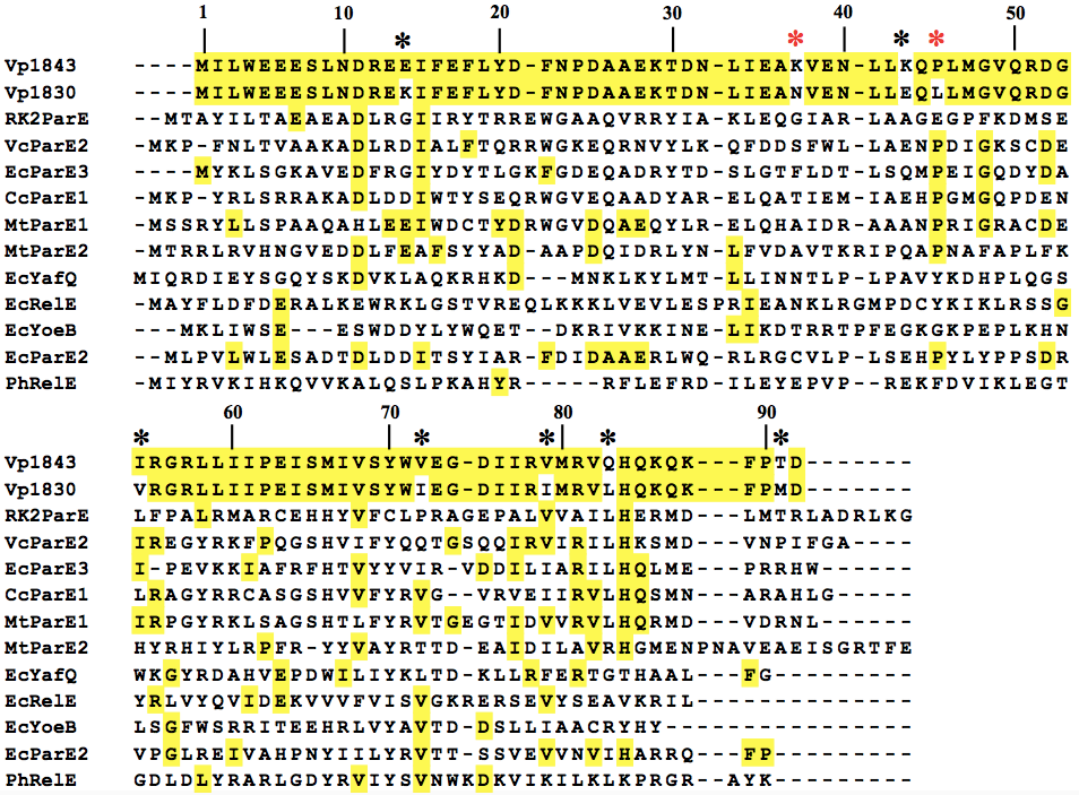

Fig. 1-7. Alignment of the amino acid sequence of toxic proteins belonging to the RelE/ParE superfamily proteins.

The amino acids were aligned by the computer program Clustal W to maximize the homology for all proteins. Vp1843 (UniProKB Q87NM5) and Vp1830 (UniprotKB Q87NN8) are gene products in *V. parahaemolyticus* (Hino et al., 2014). RK2ParE, VcParE, EcParE2, EcParE3, CcParE, MtParE1, MtParE2, EcYafQ, EcRelE, EcYoeB, and PhRelE indicate amino acid sequences of RK2 encoded ParE (UniProtKB Q79EC5), *V. cholera* ParE2 (UniProtKB Q9KMJ0), *E. coli* ParE2 (UniProtKB Q8X366), *E. coli* ParE3 (UniProtKB Q8XE95), *C. caulobacter* ParE (UniProtKB Q9A9T8), *M. tuberculosis* ParE1 (UniProtKB P9WHG7), *M. tuberculosis* ParE2 (UniProtKB P9WHG5), *E. coli* YafQ (UniProtKB Q47149), *E. coli* RelE (UniPtotKB P0C077), *E. coli* YoeB (UniProtKB P69348), and *Pyrococcus horikoshii* RelE (UniProtKB O73966), respectively. Amino acid residues are numbered according to the *V. parahaemolyticus* Vp1843. Amino acids identical to those in Vp1843 are in yellow. * indicate different amino acids between Vp1843 and Vp1830. The essential amino acids Lys37 and Pro45 for Gyr inhibitory activity of Vp1843 is indicated in red.

fact that the toxins belonging to this family share a low similarity in primary structure and display distinct biochemical activities. Namely, the RelE type toxins, such as YafQ and YoeB, stall the ribosome by cleaving mRNA in a translation-dependent fashion (Masuda et al., 2012). Recent structural studies of the ribosome in complex with RelE or YoeB provided insight into the structural basis for ribosome-dependent ribonuclease activity and suggested catalytic residues in individual toxins (Aakre et al., 2013; Christensen et al., 2001). On the other hand, ParE was originally found on plasmid RK2 with ParD being the antitoxin, and DNA gyrase (Gyr) was identified as its target molecule (Wang et al., 2013). Subsequently, several ParE genes have been found on bacterial chromosomal DNA, and biochemical studies reported that the ParE type toxins strongly poison Gyr. However, the molecular mechanism by which ParE toxins

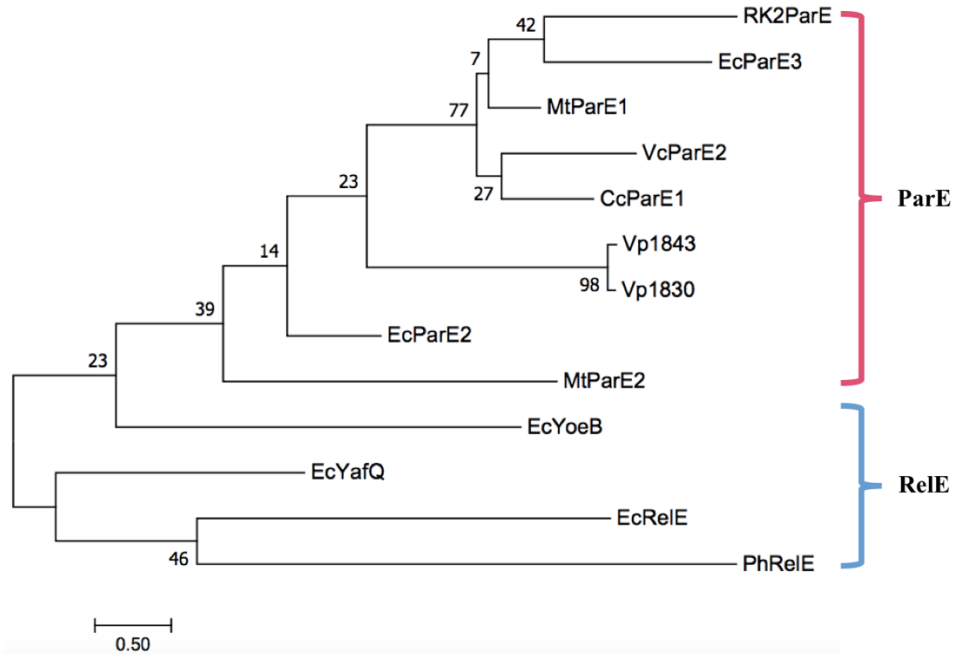

Fig. 1-8. Evolutionary relationship of RelE/ParE superfamily toxins.

Based on the amino acid sequence comparison shown in Fig.1-7, an evolutionary tree for the RelE/ParE superfamily toxins was constructed. This evolutionary tree shows that the ParE toxins (red), such as Vp1843, are clearly separated from the RelE toxins (blue), such as YafQ and YoeB, with protein synthesis inhibitory activity.

inhibit Gyr has not yet been elucidated (Sterckx et al., 2016; Yuan et al., 2010; Gupta et al., 2016).

In this study, to gain insight into biological properties of Vp1842/Vp1843, inhibitory potency of Vp1843 was first investigated with *E. coli* Gyr. As described in Chapter 2, I found that it, unlike other ParE toxins, had little inhibitory activity toward Gyr. Rather, Vp1843 exhibited DNA endonuclease activity. Next, I examined whether *vp1842/vp1843* is involved in induction into the VBNC state by preparing a mutant strain (Δ*vp1842/vp1843*), in which *vp1842/vp1843* in the *V. parahaemolyticus* genome was knocked out by homologous recombination. As described in Chapter 3, Δ*vp1842/vp1843* entered into the VBNC state at a comparable rate with that of the wild-type. Furthermore, a preliminary transcriptome analysis using next generation sequence showed that the *vp1842/vp1843* transcript in the VBNC state was comparable with that in normal growth conditions. It is thus likely that *vp1842/vp1843* is not involved in the induction into the VBNC state. In order to gain insight into physiological functions of *vp1842/vp1843*, *E. coli cells*, in which *vp1843* was expressed, were characterized in terms of phenotypic properties using flow cytometry and microscopic analysis. I found that expression of *vp1843* caused extreme degradation of the chromosomal DNA, as described in Chapter 4. Finally, I discuss a possible physiological role of *vp1842/vp1843* in *V. parahaemolyticus* on the basis of biological information obtained in this study, as described in Chapter 5.

Chapter 2

Biological activity of Vp1843

2-1. Introduction

Phylogenetic studies have found that Vp1843 belongs to the RelE/ParE superfamily. Toxins belonging to this family fold into a similar fold while they display distinct physiological functions (Fig. 2-1). That is, the RelE toxins, such as RelE and YafQ, inhibit protein synthesis by cleaving mRNA (mRNA inteferase), while the ParE toxins have an inhibitory activity towards DNA gyrase (Gyr). However, their molecular mechanism remains unclear. Namely, the crystal structure of the *E. coli* RelE in complex with the *Thermus thermophilus* ribosome revealed that Arg81 and Tyr87 play an essential role in mRNA interferase activity as a general acid and base, respectively (Neubauer et al., 2009). On the other hand, structural and biochemical studies on YafQ found that His50, His63, Asp67 and His87 participate in acid-base catalysis during mRNA hydrolysis and further suggested that Phe91 plays an important role in mRNA positioning (Maehigashi et al., 2015). Collectively, catalytic residues in RelE and YafQ are not conserved, and their catalytic mechanism has not been fully understood.

As for ParE toxins, it has been reported that they have an inhibitory activity towards DNA gyrase (Gyr). Gyr is the only type II topoisomerases capable of introducing negative supercoils at the expense of ATP hydrolysis (Gubaev et al., 2016; Gellert et al., 1976). In addition, Gyr is able to relax supercoiled DNA in the absence of ATP (Fig. 2-2) (Gellert et al., 1976). Gyr consists of two subunits, GyrA and GyrB (97 kDa and 90 kDa, respectively, in *E. coli*) and forms a heterotetramer $GyrA_2GyrB_2$ in the active enzyme. The ParE toxins from different bacteria inhibit DNA gyrase in a different mechanism. First, RK2 plasmid ParE and *V. cholerae* ParE2 stabilize the cleavage complex by interacting with Gyr A subunit (GyrA), despite having distinct binding sites (Jiang et al., 2002; Yuan et al., 2010). Second, *Mycobacterium turbaclosis* ParE inhibits Gyr by interacting with Gyr B subunit (GyrB), the C-terminal residues being suggested

to be involved in the inhibitory activity (Gupta et al., 2016). Third, *E. coli* ParE2 interacts with neither GyrA nor GyrB, although its Gyr inhibitory activity has not been experimentally verified (Sterckx et al., 2016). As described above, the molecular mechanism by which ParE toxins inhibit Gyr has not been fully elucidated.

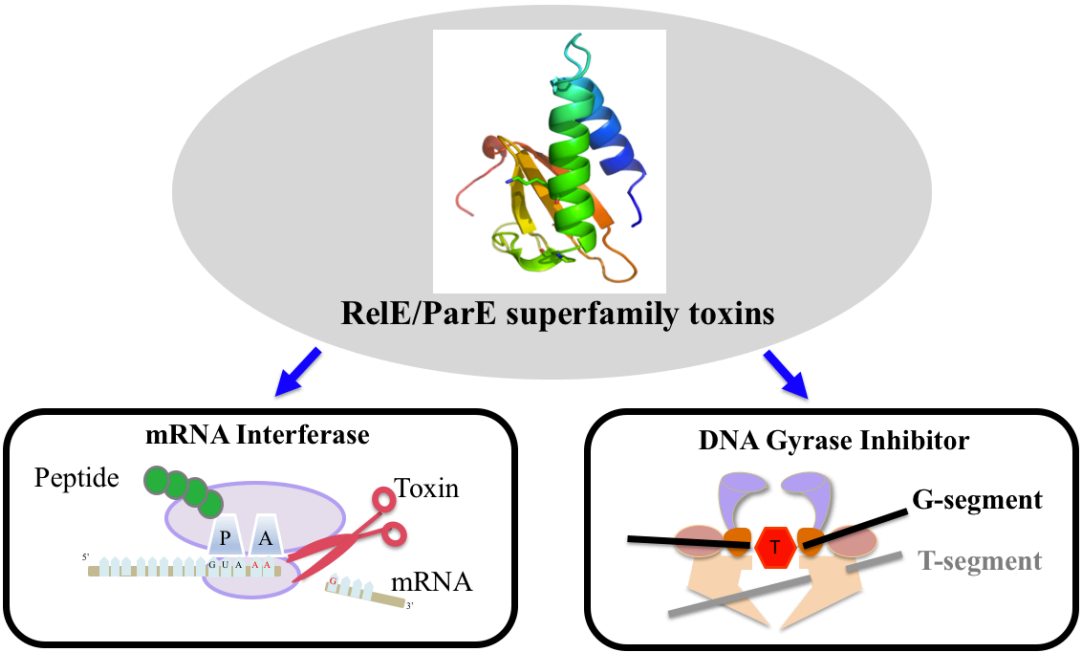

Fig. 2-1. Functions of toxins belonging to the RelE/ParE superfamily.

Toxins which belong to the RelE/ParE superfamily fold into a similar fold, while they display two distinct biochemical activities. The RelE family toxins, such as YafQ and YoeB, stall the ribosome by cleaving mRNA (mRNA interferase), while the ParE family toxins have been reported to interfere with DNA replication by inhibiting DNA gyrase.

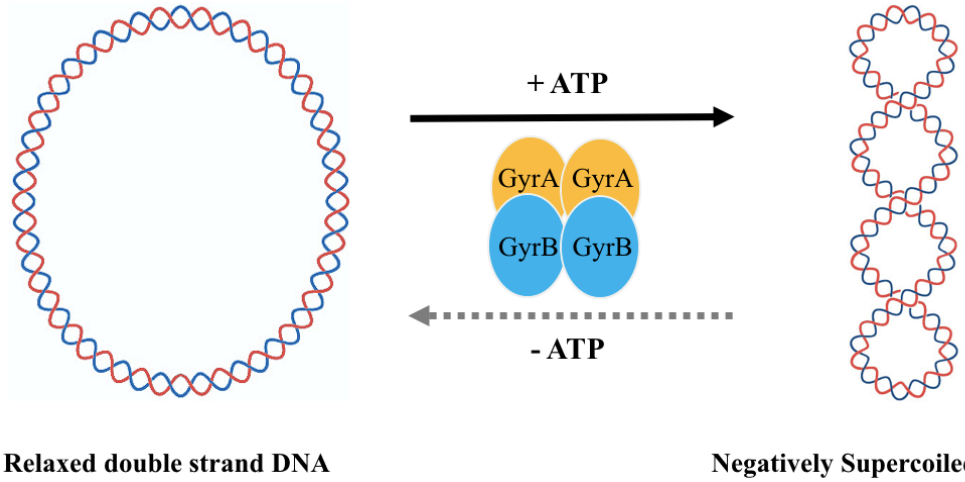

Fig. 2-2. Catalytic activities of DNA gyrase.

In the presence of ATP, Gyr ($GyrA_2GyrB_2$) is able to convert relaxed DNA into supercoiled DNA. However, in the absence of ATP, Gyr ($GyrA_2GyrB_2$) relaxes the supercoiled DNA in a relatively low activity.

Our previous study showed that Vp1843 has neither mRNA cleavage activity nor protein synthesis inhibition activity (Hino et al., 2014). To gain more insight into the biological properties of Vp1842/Vp1843, I investigated the inhibitory potency of Vp1843 with *E. coli* Gyr.

2-2. Materials and Methods

2-2-1. Materials

Restriction endonucleases and DNA modifying enzymes were purchased from MBI Fermentas. The *E. coli* Gyr was supplied by New England Biolabs. Oligonucleotides used in this study were purchased from Operon. Ciprofloxacin (CFX) was obtained as hydrochlorides from Enzo Life Sciences. All other chemicals were of analytical grade for biochemical use.

2-2-2. Plasmids

The relaxed plasmids, pBR322 and pUC19, were supplied by Inspiralis and New England Biolabs. The plasmid vectors pET-15b, pET22b, and pBAD/Myc-HisA used for expression of *vp1842*/*Vp1843* in *E. coli* cells were from Novagen and Invitrogen, respectively.

Plasmids for expression and purification of Vp1843-His and Vp1843 mutants (K37N, P45L, K37N/P45L) were constructed as follows. First, the *vp1842/vp1843* fragment was amplified using primer 22b-1843-NdeI-F and XhoI-1843-R and ligated into pET22b after treatment by *Nde* I and *Xho* I. Second, the resulting plasmid pET22b-*vp1842/vp1843* was used as a template for mutagenesis PCR to obtain pET22b-*vp1842/vp1843*-K37N (Primers: pET22b-4243-K37N-F and pET22b-4243-K37N-R), pET22b-*vp1842/vp1843*-P45L (Primers: pET22b-4243-K37N-F and pET22b-4243-K37N-R). pET22b-*vp1842/vp1843*-K37N/P45L was constructed with a template of pET22b-*vp1842/vp1843*-P45L and primers of pET22b-*vp1842/vp1843*-K37N-F and pET22b-*vp1842/vp1843*-K37N-R. Third, a *vp1843*-K37N/P45L fragment was amplified using pET22b-*vp1842/vp1843*-K37N/P45L as a template with primers 22b-1843-NdeI-F and XhoI-1843-R, and ligated into pET22b with *Nde* I and *Xho* I digestion. The resulting plasmid pET22b-*vp1843*-K37N/P45L was used for expression and purification of K37N/P45L. Primers were listed in Table 2-1.

Plasmids for examination of toxicity of Vp1843 and its mutants (K37N, P45L, K37N/P45L) were constructed as follows. Gene fragments of *vp1843, vp1843*-K37N, *vp1843*-P45L and *vp1843*-K37N/P45L were amplified using the primer pair of pBAD-1843-NcoI-F and pBAD-1843-HindIII-R with their corresponding templates pET22b-*vp1842/vp1843,* pET22b-*vp1842/vp1843*-K37N, pET22b-*vp1842/vp1843*-P45L and pET22b-*vp1843*-K37N/P45L. These fragments were ligated into pBAD-Myc-HisA in the aid of *Nco* I and *Hind* III digestion, resulting in three plasmids pBAD-*vp1843,* pBAD-*vp1843*-K37N, pBAD-*vp1843*-P45L and pBAD-*vp1843*-K37N/P45L. Sequences of the primers were listed in Table 2-1.

Table 2-1. Oligonucleotide used in this study

Oligonucleotide	Sequence (5'-3')
22b-1843-NdeI-F	5'-TCGAGGTAACATATGATTTTATGGGAAGAA-3'
XhoI-1843-R	5'-AAGAAGCTCGAGATCCGTAGGGAATTT-3'
pET22b-4243-K37N-F	5'ATTGAAGCAAACGTAGAAAACTTGCTTAAACAACC-3'
pET22b-4243-K37N-R	5'-GTTTTCTACGTTTGCTTCAATGAGGTTGTCAGTTT-3'
pET22b-4243-P45L-F	5'-AAACAACTTTTAATGGGTGTGCAACGAGATGGCAT-3'
pET22b-4243-P45L-R	5'-ACACCCATTAAAAGTTGTTTAAGCAAGTTTTCTAC-3'
pBAD-1843-NcoI-F	5'-GTAATCGACCATGGATATGATTTTATGGGAAG-3'
pBAD-1843-HindIII-R	5'-AGAGGAAGCTTTCAGTGGTGGTGGTGGTG-3'

2-2-3. Strains

The *E. coli* strain JM109 was used as a host cell for cloning, and *E. coli* strains BL21(DE3) Codon Plus RIL (Stratagene) and LMG194 (Invitrogen) were used as host cells for the expression of recombinant proteins.

2-2-4. Protein purification

For purification of Vp1843 or Vp1843-His, the His-Vp1842/Vp1843 or Vp1842/Vp1843-His complex was purified by affinity column chromatography on a COSOMOGEL His-Accept column. Then, they were treated by 6 M guanidine hydrochloride and loaded onto a COSOMOGEL His-Accept column to separate His-Vp1842 from His-Vp1842/Vp1843 or Vp1843-His from Vp1842/Vp1843-His. The Vp1843 protein solution was dialyzed against 50 mM Tris-HCl, pH 8.0, containing 500 mM NaCl and 400 mM arginine hydrochloride at 4°C overnight and finally against 50 mM Tris-HCl, pH 7.5, containing 100 mM NaCl. Then, the protein solution was concentrated using Amicon® Ultra Centrifugal Filters Ulteracel-3K (Merck Millipore Ltd). Vp1843-His was refolded in a HisTrap column (GE healthcare) by 20 column volumes buffer containing 50 mM Tris-HCl, pH 8.0, 500 mM NaCl, 10% glycerol and 0.02% tween20 in a liner gradient from 0% to 100%. After eluting the refolded Vp1843-His by 50 mM Tris-HCl, pH 8.0, 500 mM NaCl, 10% glycerol, 0.02% tween20, and 400 mM Imidazole, it was further diluted and applied to a HitrapQ column (GE healthcare). The HitrapQ column was washed by 50 mM Tris-HCl, pH 8.0, 50 mM NaCl, 10% glycerol and 0.5mM DTT and then protein was eluted by increasing NaCl concentration from 50 mM to 1.0 M in the same buffer. After collecting the fractions containing Vp1843-His and checking by 15% SDS-PAGE, the protein was dialysis against 50 mM Tris-HCl, pH 7.5, containing 100 mM NaCl. Finally, the protein solution was concentrated using Amicon® Ultra Centrifugal Filters Ulteracel-3K (Merck Millipore Ltd). Mutant proteins were purified in the same manner, as described above.

2-2-5. *E. coli* Gyr inhibitory activity

Gyr inhibitory assays were carried out as described previously (Sterckx et al., 2016; Yuan et al., 2010). Inhibitory activity toward Gyr supercoiling was carried out as follows. Relaxed pBR322 (400 ng) or pUC19 (400 ng) was mixed with 2 units of Gyr in the presence or absence of increasing amounts of Vp1843 (1 ~ 5 μM) or CFX (1 ~ 5 μM) in a reaction buffer containing 35 mM Tris-HCl, 24 mM KCl, 4 mM $MgCl_2$, 2 mM DTT, 5 mM spermidine, 1.75 mM ATP, 6.5% glycerol, and 0.1 mg/mL BSA. As for inhibitory activity toward Gyr relaxation, the supercoiled DNA was incubated in the same manner as those described above, except that the reaction buffer without ATP was used. After incubating the reactions at 25°C for 4 h, the mixtures were treated by a stop buffer containing SDS (0.2%) and proteinase K (1 mg/mL) at 37°C for 30 min. The DNA products were analyzed by electrophoresis in a 1% agarose gel in TAE buffer and visualized by ethidium bromide.

2-2-6. DNA nicking endonuclease activity

Relaxed or supercoiled pUC19 (100 ng) or pBR322 (100 ng) was incubated with Vp1843-His (0 ~ 5 μM), its mutants (0 ~ 5 μM), or Vp1842/Vp1843-His (0 ~ 5μM), in a reaction buffer containing 25 mM Tris-HCl, 20 mM NaCl, 4 mM $MgCl_2$, 2 mM β-ME, and 6.5% glycerol. The total reaction volume was adjusted to 10 μl. After incubating the reactions at 25°C for 4 h, the DNA products were released by 0.2% SDS and 1 mg/mL Protease K treatment at 37°C for 30 min and then analyzed by electrophoresis in a 1% agarose gel in TAE and visualized by ethidium bromide. For separation of relaxed form DNA from open-circular DNA with nicks, the reaction products were analyzed by electrophoresis in a 1% agarose gel in TBE, as described previously (Lee *et al*., 2015). To examine divalent metal ion preference, the nicking activity was measured in the same manner as those described above, except that $MgCl_2$ was replaced by $MnCl_2$ or $CaCl_2$ in the reaction buffer.

2-3. Results

2-3-1. Purification of Vp1843

E. coli strain BL21(DE3) Codon Plus RIL harboring pET15b-*vp1842/vp1843* or pET22b-*vp1842/vp1843* was cultured to log-phase in LB medium (1L). Expression of *vp1842/vp1843* was induced by 1 M IPTG at 25°C for 20 h. Cells (5 ~ 6 g) were collected and re-suspended in 100 ml sonication buffer containing 50 mM Tris-HCl, pH 8.0, 500 mM NaCl. After sonication at a mode of (pulse-on for 10 seconds following by pulse-off for 40 seconds with an amplitude of 50) in a progress of 6 min, the supernatant containing total proteins was obtained by centrifuging at 4°C in a speed of 35,000 g for 30 min. Vp1842/Vp1843-His, Vp1843 and Vp1843-His were purified as described in Materials and Methods. The purified samples were applied to 15% SDS-PAGE and electrophoresis at 30 mA for 1 h (Fig. 2-3). The yields of Vp1843 and Vp1843-His were 0.5 mg/L and 4 mg/L, respectively.

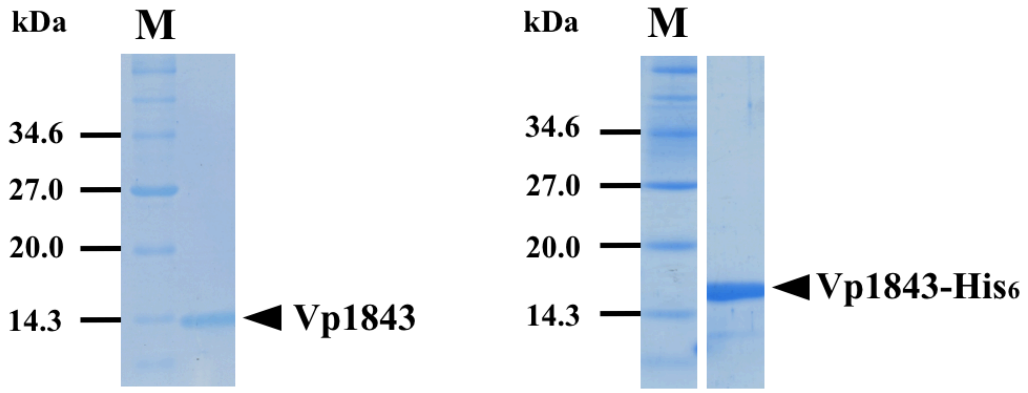

Fig. 2-3. Purification of Vp1843 without His_6 (left) or with His_6 (right).

The toxin Vp1843 was purified as described in Materials and Methods and analyzed by 15% SDS-PAGE. Arrows indicate the location of Vp1843 without His_6 (left) or with His_6 (right). M indicates the protein markers, bands of 14.3 kDa, 20.0 kDa, 27.0 kDa and 34.6 kDa stand for lysozyme (chiken egg white), trypsin inhibitor (Soybean), triosephosphate isomerase (*E. coli*) and thioredoxin reductase (*E. coli*), respectively.

2-3-2. Gyr inhibitory activity

Vp1843 has sequence homology not only to *E. coli* YafQ, but also to *C. crescentus* ParE, as shown in Fig. 1-7. Both YafQ and ParE toxins belong to the RelE/ParE superfamily, despite distinct biological activities; YafQ is a protein synthesis inhibitor by cleaving mRNA (Griffin et al., 2013), while ParE has inhibitory activity toward Gyr (Jiang et al., 2012). Since Vp1843 exhibited neither protein synthesis inhibitory activity nor ribonuclease activity (Hino et al., 2014), I tested whether Vp1843 could have any inhibitory activity toward *E. coli* Gyr using ciprofloxacin (CFX) as a control. In this assay, mixtures containing relaxed pBR322 and Gyr were incubated with an increasing amount of Vp1843 (0 ~ 5 μM) or CFX (0 ~ 5 μM) at 25°C for 4 h, and then, the reaction mixtures were treated with SDS and Proteinase K to detect the Gyr-DNA cleavage

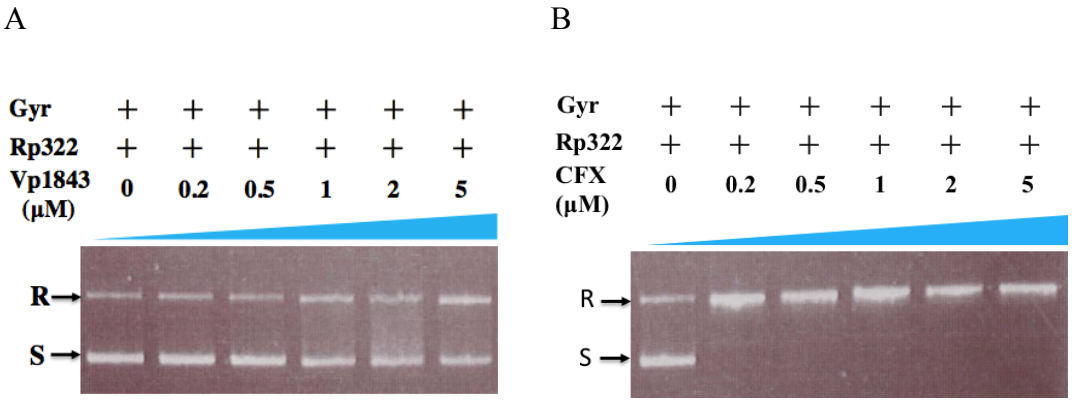

Fig. 2-4. Influence of Vp1843 (A) or CFX (B) on the supercoiling activity of Gyr.

Relaxed pBR322 (200 ng) was mixed with 2 units of Gyr in the presence of Vp1843 (0 ~ 5 μM) (A) or CFX (0 ~ 5 μM) (B) in a reaction buffer containing 35 mM Tris-HCl, 24 mM KCl, 4 mM $MgCl_2$, 2 mM DTT, 5 mM spermidine, 1.75 mM ATP, 6.5% glycerol, and 0.1 mg/mL BSA. After incubating the reactions at 25°C for 4 h, the mixtures were treated with stop buffer containing SDS (0.2%) and Proteinase K (1 mg/mL) at 37°C for 30 min. The DNA products were analyzed by electrophoresis on a 1% agarose gel in TAE buffer and visualized by ethidium bromide. Rp322, relaxed pBR322; R, relaxed pBR322; S, supercoiled pBR322.

complex on agarose gels, as described previously (Sterckx et al., 2016; Yuan et al., 2010). The result showed that Vp1843 appeared to inhibit the supercoiling activity of

Gyr slightly at 25°C for 4 h, accumulating relaxed form DNA in a dose-dependent manner (Fig. 2-4A). However, its inhibitory activity was considerably weaker than CFX (Fig. 2-4B).

Since it is known that Gyr catalyzes not only DNA supercoiling in the presence of ATP, but also DNA relaxation of supercoiled DNA in the absence of ATP (Collin et al., 2011), I tested whether Vp1843 could inhibit the DNA relaxation activity of Gyr using supercoiled pBR322 as a substrate. In this analysis, the supercoiled pBR322 treated with Gyr was incubated with an increasing amount of Vp1843 (0 ~ 5 μM) or CFX (0 ~ 5 μM) at 25°C for 4 h and then, the reaction mixtures were analyzed as described above. Interestingly, Vp1843 appeared to enhance the Gyr relaxation activity, showing that the dose-dependent decrease of the supercoiled DNA was concomitant

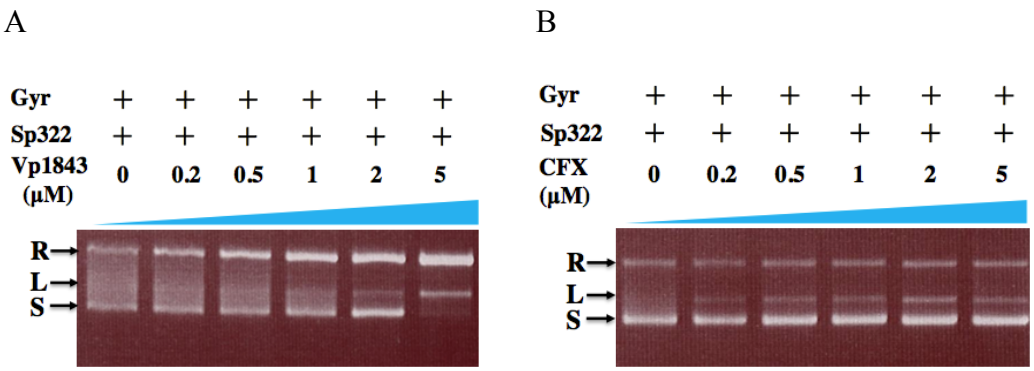

Fig. 2-5. Influence of Vp1843 (A) or CFX (B) on the relaxation activity of Gyr.

Supercoiled pBR322 (200 ng) was mixed with 2 units of Gyr in the presence of Vp1843 (0 ~ 5 μM) (A) or CFX (0 ~ 5 μM) (B) in a reaction buffer containing 35 mM Tris-HCl, 24 mM KCl, 4 mM $MgCl_2$, 2 mM DTT, 5 mM spermidine, 1.75 mM ATP, 6.5% glycerol, and 0.1 mg/mL BSA. After incubating the reactions at 25°C for 4 h, the mixtures were treated with stop buffer containing SDS (0.2%) and Proteinase K (1 mg/mL) at 37°C for 30 min. The DNA products were analyzed by electrophoresis on a 1% agarose gel in TAE buffer and visualized by ethidium bromide.

with the increase of the relaxed form DNA (Fig. 2-5A). In contrast, CFX inhibited the relaxation activity of Gyr (Fig. 2-5B). This result led me to the speculation that Vp1843 has no influence on the DNA relaxation activity of Gyr, rather it converts the

supercoiled DNA to the relaxed DNA (or open-circular DNA) with nicks by a DNA nicking endonuclease activity.

2-3-3. Vp1843 has a DNA nicking activity

Next, I tested if Vp1843 could convert supercoiled DNA to relaxed DNA (or open-circular DNA) in the absence of Gyr. As expected, Vp1843 alone completely converted supercoiled DNA to relaxed DNA (or open-circular DNA), giving rise linear DNA in a dose-dependent manner (Fig. 2-6).

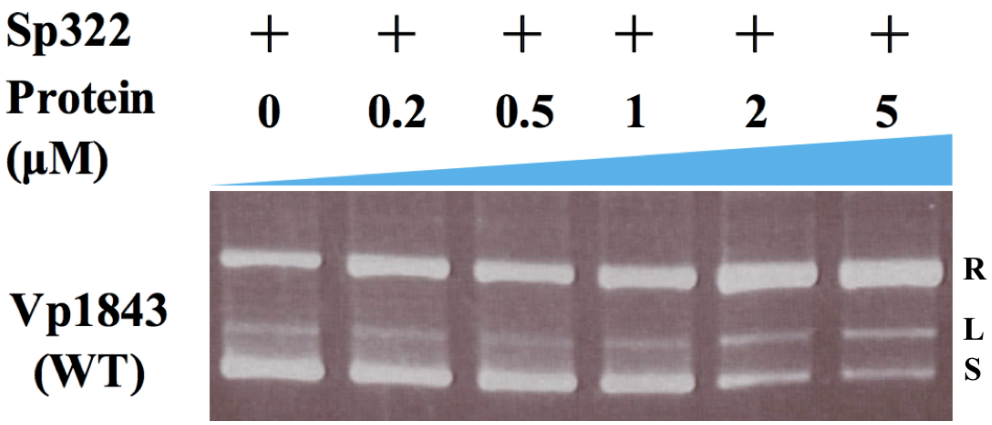

Fig. 2-6. DNA nicking endonuclease activity of Vp1843.

Supercoiled pBR322 (100 ng) was incubated with Vp1843 (0 ~ 5 μM) in a nicking reaction buffer containing 25 mM Tris-HCl, pH 7.5, 20 mM NaCl, 4 mM $MnCl_2$, 2 mM β-ME, and 6.5% glycerol in 10 μl reaction system. After incubating the reactions at 25°C for 4 h, the DNA products were released by 0.2% SDS and 1 mg/mL Protease K treatment at 37°C for 30 min and then analyzed by electrophoresis on a 1% agarose gel in TAE buffer at 100 V for 50 min and visualized by ethidium bromide. R, L, S stand for relaxed, linear and supercoiled DNA, respectively.

To further corroborate the nicking endonuclease activity of Vp1843, the reaction products were analyzed on 1% agarose gel in TBE buffer instead of TAE buffer, because this gel electrophoresis in TBE buffer is known to separate open-circular DNA

with nicks from relaxed form DNA without nicks, as described previously (Lee et al., 2015). In this electrophoresis, nicked open-circular DNA with one strand cut, relaxed circular DNA without nicks, and linear DNA with free ends are the slowest to the fastest in order of electrophoretic mobility (Lee et al., 2015). As shown in Fig. 2-7, Vp1843 could convert both relaxed form DNA (lane 3) and supercoiled DNA (lane 4) to open-circular DNA, accumulating linearized DNA. I further found that prolong incubation of supercoiled DNA with Vp1843 did not increase the linear products (data not shown), suggesting that the dose-dependent appearance of liner DNA is caused by single-stranded cuts at close sites on opposite strands.

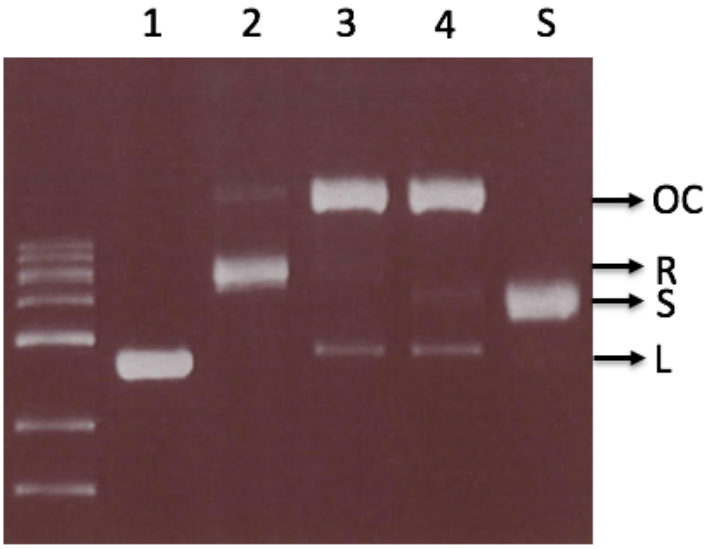

Fig. 2-7. Agarose gel electroporesis of open-circular DNA and relaxed DNA.

Supercoiled pUC19 (100 ng) and relaxed pUC19 (100 ng) was incubated with 5 μM Vp1843 at 25°C for 4 h in the same buffer as in Fig. 2-5, and analyzed by electrophoresis on a 1% agarose gel in TBE buffer at 100 V for 90 min. Lane1, linearized pUC19 by EcoRI; lane 2, relaxed pUC19; lane 3, relaxed pUC19 incubated with Vp1843; lane 4, supercoiled pUC19 incubated with Vp1843; lane 5, supercoiled pUC19. Sp322 indicates supercoiled pBR322, and S, L, R, OC stand for supercoiled, linear, relaxed and open circular DNA, respectively.

2-3-4. Characterization of the nicking activity of Vp1843

As described previously, the *E. coli* cell growth inhibition by Vp1843 was neutralized by expression of the antitoxin gene *vp1842* (Hino et al., 2014). Therefore, I tested whether the antitoxin Vp1842 could influence the Vp1843 nicking activity. The result showed that Vp1842 could neutralize the nicking activity of Vp1843, although linearized DNA slightly accumulated in a dose dependent manner (Fig. 2-8).

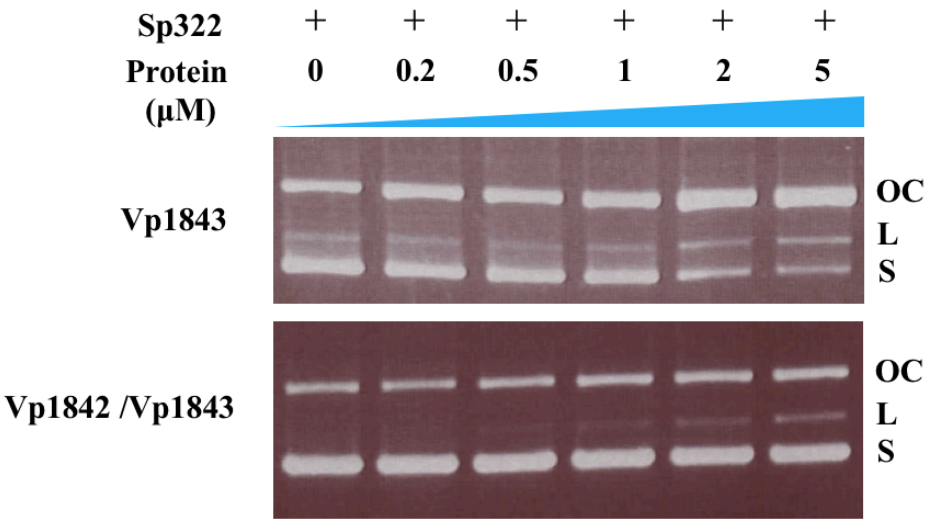

Fig. 2-8. Vp1842 neutralize the DNA nicking endonuclease activity of Vp1843.

Supercoiled pBR322 (100 ng) was incubated with Vp1843 or Vp1842/Vp1843 (0 ~ 5 μM) in a nicking reaction buffer containing 25 mM Tris-HCl, pH 7.5, 20 mM NaCl, 4 mM $MnCl_2$, 2 mM β-ME, and 6.5% glycerol in 10 μl reaction system. After incubating the reactions at 25°C for 4 h, the DNA products were released by 0.2% SDS and 1 mg/mL Protease K treatment at 37°C for 30 min and then analyzed by electrophoresis on a 1% agarose gel in TAE buffer at 100 V for 50 min and visualized by ethidium bromide. O, L, S stand for open circular, linear and supercoiled DNA, respectively.

This finding is consistent with the fact that the co-expression of *vp1842* and *vp1843* slightly influenced the *E. coli* cell growth as compared with that of *E. coli* cells ontaining pBAD/Myc-HisA (Hino et al., 2014). Nevertheless, the result indicates that the strong toxicity of Vp1843 in *E. coli* is attributable to DNA damage by its nicking activity.

It is known that almost all DNA nicking endonucleases exhibit catalytic activity in the presence of a divalent metal ion (Pingoud et al., 2014; Xu., 2015). The reaction buffer used for the nicking activity for Vp1843 contained 4 mM Mg^{2+}. I first examined whether Vp1843 requires Mg^{2+} ion for its enzymatic activity. As shown in Fig. 2-9, although Vp1843 converts supercoiled pBR322 to relaxed DNA in the presence of

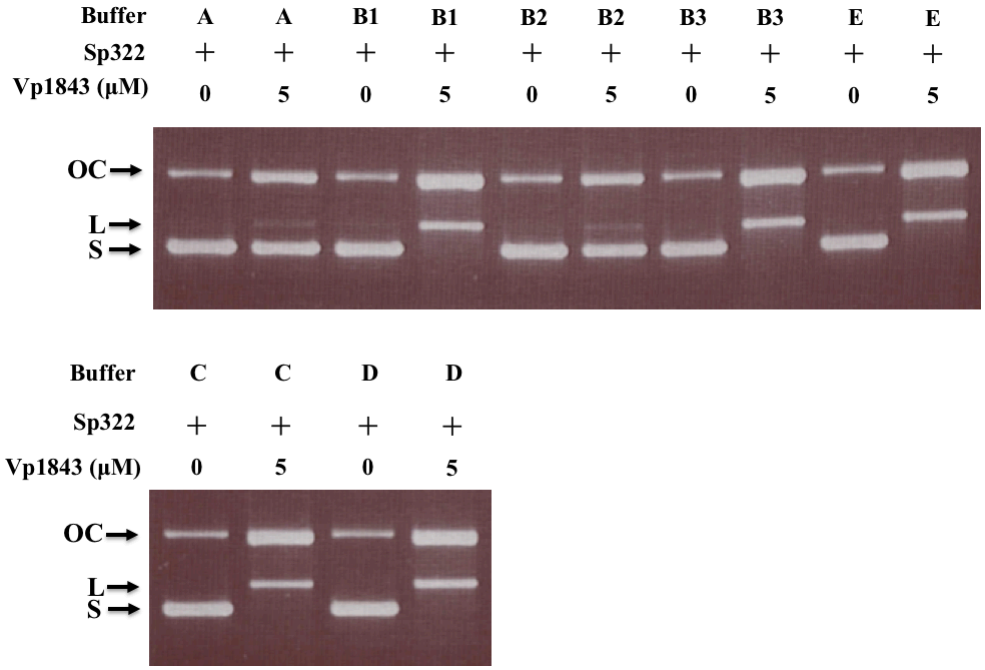

Fig. 2-9. Vp1843's nick activity needs divalent Mg^{2+}.

Vp1843 (5 μM) was incubated with 100 ng supercoiled pBR322 in different buffers, containing Na^{+} or K^{+} or Mg^{2+}. Reaction conditions are the same as in materials and methods. Buffer A: 25 mM Tris-HCl, pH 7.5 and 20 mM NaCl; B1: 25 mM Tris-HCl, pH 7.5, 20 mM NaCl and 20 mM $MgCl_2$; B2: 25 mM Tris-HCl, pH 7.5 and 20 mM KCl; B3: 25 mM Tris-HCl, pH 7.5, 20 mM KCl and 20 mM $MgCl_2$; C: 25 mM Tris-HCl, pH 7.5, 20 mM NaCl and 20 mM $MgCl_2$, 2 mM β-ME; D: 25 mM Tris-HCl, pH 7.5, 20 mM NaCl and 20 mM $MgCl_2$, 2 mM β-ME, 6.5% glycerol; E: 25 mM Tris-HCl, pH 7.5, 20 mM KCl and 20 mM $MgCl_2$, 2 mM β-ME, 6.5% glycerol. Sp322, supercoiled pBR322; OC, open circular DNA; L, linearized DNA; S, supercoiled DNA.

Mg^{2+}, no conversion from supercoiled DNA to relaxed DNA was detected in the absence of Mg^{2+}, demonstrating requirement of Mg^{2+} for the enzymatic activity of Vp1843.

Next, we tested preference of divalent metal ions for the Vp1843 activity using $MnCl_2$ and $CaCl_2$ in place of $MgCl_2$. Vp1843 completely converted supercoiled pBR322 to open-circular DNA generating a small amount of linear DNA in the presence of Mn^{2+}, while supercoiled DNA was partially converted to open-circle DNA in the presence of Ca^{2+}, indicating that Vp1843 efficiently nicks DNA in the presence of a divalent ion in the order of $Mn^{2+} > Mg^{2+} > Ca^{2+}$ (Fig. 2-10).

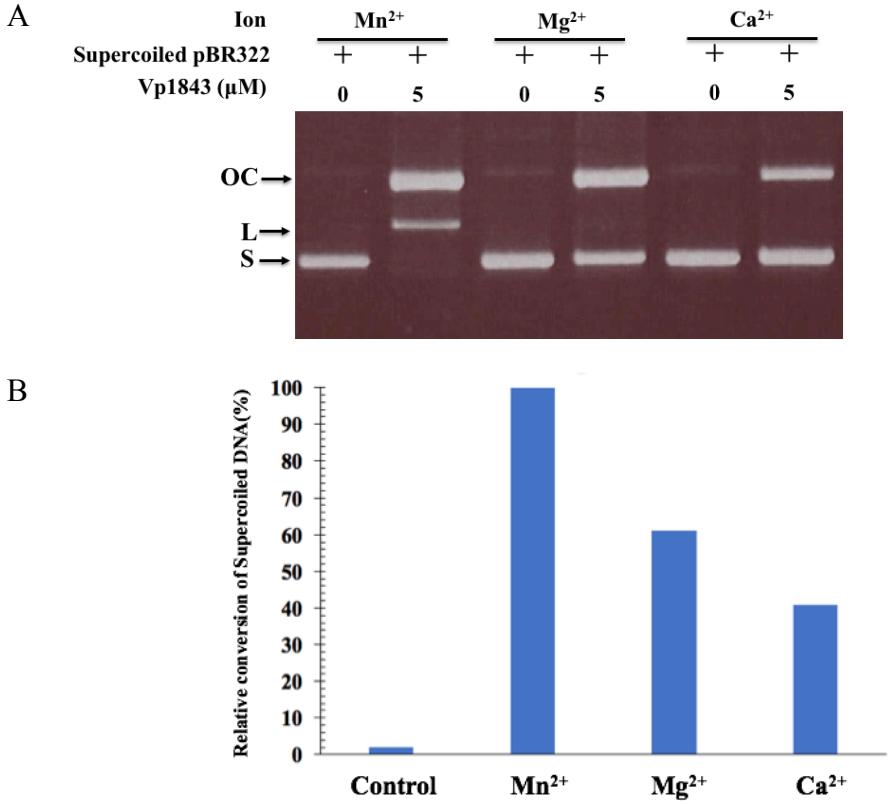

Fig. 2-10. Ion preference of Vp1843.

(A) Supercoiled pBR322 (100 ng) was incubated with Vp1843 (5 μM) or without Vp1843 (as a control) in a nicking reaction buffer containing either $MgCl_2$, $MnCl_2$ or $CaCl_2$, and the DNA products were analyzed in the same manner as described in Materials and Methods. Sp322 indicates supercoiled pBR322, and S, L, OC stand for supercoiled, linear, and open circular DNA, respectively. (B) The relative conversion from supercoiled DNA to open-circle DNA and linear DNA were used to evaluate the activity of Vp1843. Image J software was utilized to digitalize the results of electrophoresis.

I further examined the nicking activity of Vp1843 at different pH from 5.7 to pH 8.5. The appearance of bands standing for open-circle DNA (OC) indicated that Vp1843 was active in these conditions. This result showed that the optimum pH value for Vp1843 is pH 7.0 to pH 8.5. (Fig. 2-11).

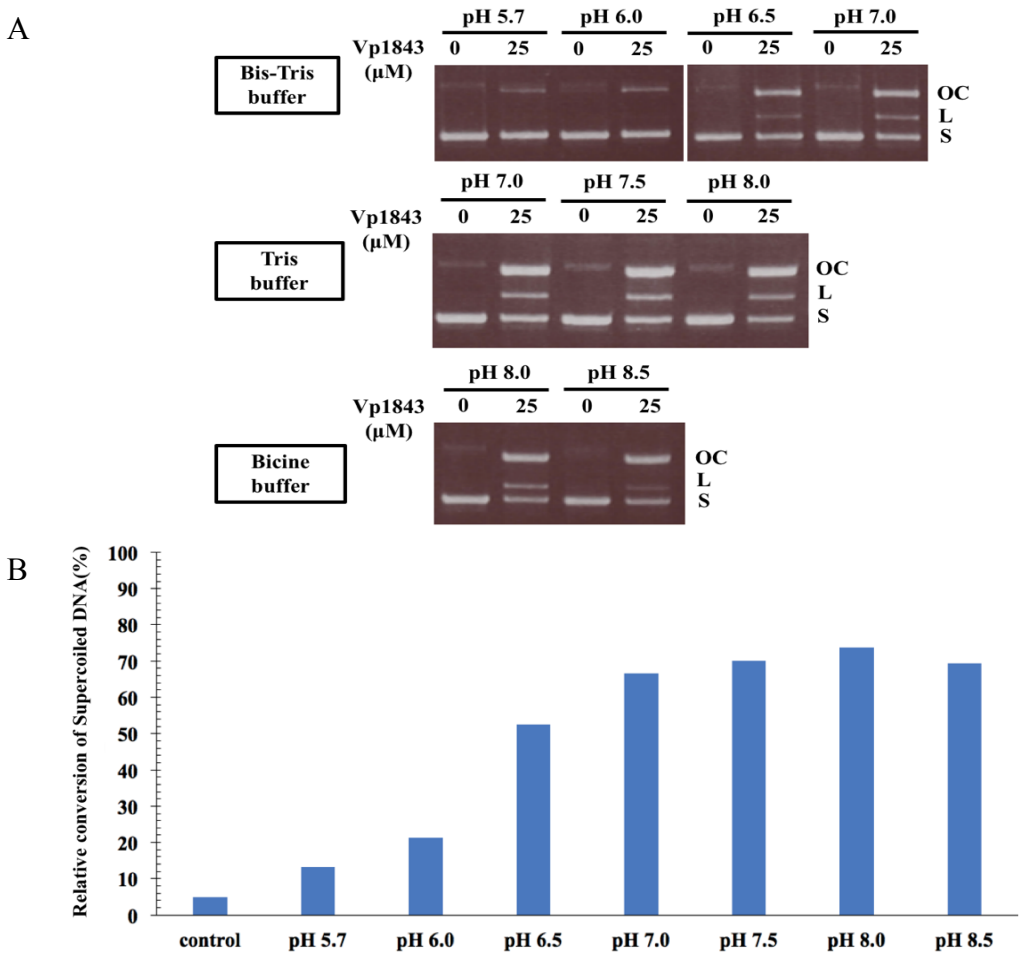

Fig. 2-11. pH dependency of the nicking activity of Vp1843.

(A) Supercoiled pBR322 (100 ng) was incubated with Vp1843 (0 μM, 25 μM) in the nicking reaction buffer with Mn^{2+} at different pH as indicated above. To exclude the possible effect of pH buffer, three kinds of pH buffer (Bis-Tris buffer, Tris buffer, Bicine buffer) were selected and examine the nicking activity of Vp1843. After incubating the reactions for 1 h, the DNA products were analyzed in the same manner as described in Materials and Methods. (B) The conversion rate of supercoiled DNA into open-circle DNA and linear DNA were used to evaluate the activity of Vp1843. The Image J software was utilized to digitalize the results of electrophoresis.

To find the optimum temperature for Vp1843, I also examined the nicking activity of Vp1843 at a temperature range from 10°C to 50°C. The result indicated that Vp1843 was active in these conditions. DNA nicking activity of Vp1843 was about 70% at 10°C, while 90% from 25°C to 50°C (Fig. 2-12), indicating the optimum temperature of Vp1843 is 25 ~ 50°C.

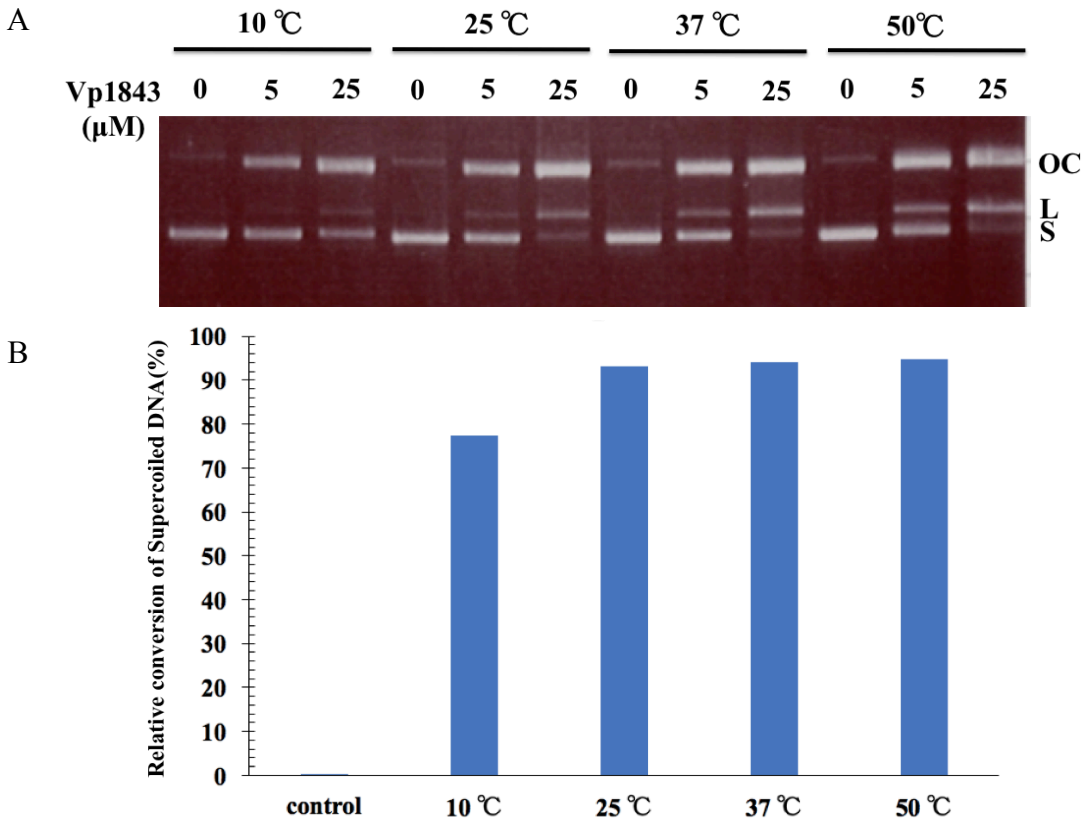

Fig. 2-12. Vp1843 is active at a variety of temperature.

(A) Supercoiled pBR322 (100 ng) was incubated with Vp1843 (0 μM, 5 μM, 25 μM) in the nicking reaction buffer with Mn^{2+} at different temperatures as indicated above. After incubating the reactions for 1 h, the DNA products were analyzed in the same manner as described in Materials and Methods. (B) The conversion rate of supercoiled DNA into open-circle DNA and linear DNA were used to evaluate the activity of Vp1843. The Image J software was utilized to digitalize the results of electrophoresis.

2-3-5. Essential residues in Vp1843

Previously, we found that the gene cluster *vp1829*/*vp1830*, a paralog of *vp1842*/*vp1843*, has significant homology to that encoding DinJ/YafQ of *E. coli* (Hino et al., 2014). However, the expressions of *vp1830* in the presence of 0.2% arabinose had no influence on cell growth, indicating that the protein Vp1830 has no toxicity, even though there are only 9 amino acid replacements between Vp1830 and Vp1843 (Fig. 1-7). The subsequent mutational analysis showed that replacing Asn37 or Leu45 in Vp1830 with the corresponding residue Lys37 or Pro45 in Vp1843 significantly

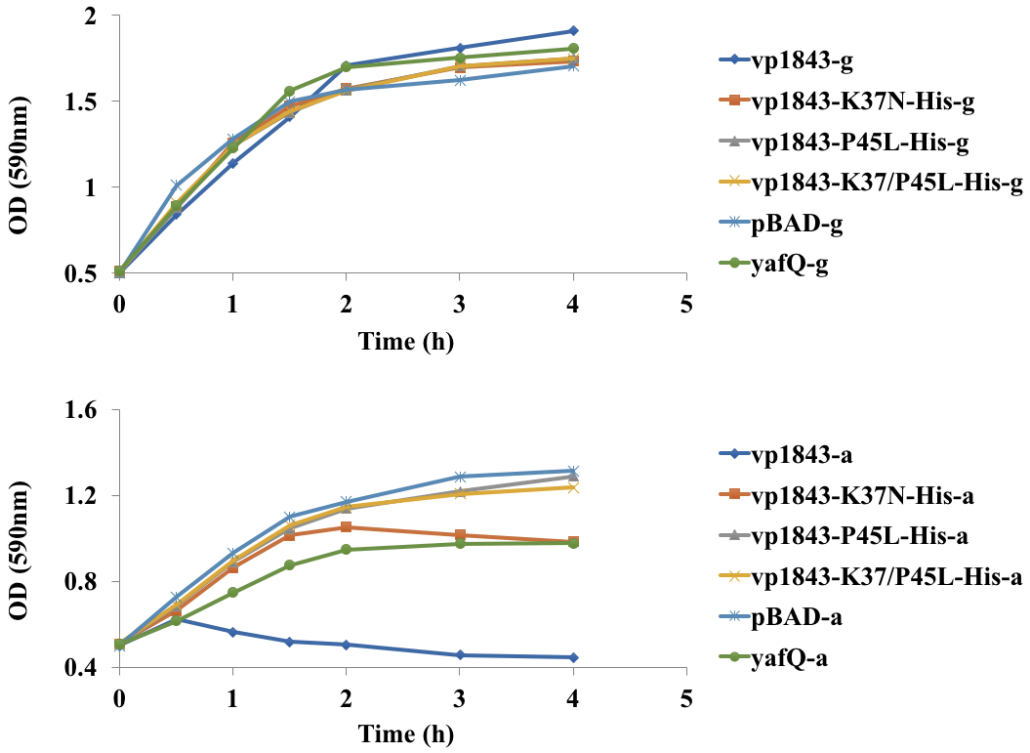

Fig. 2-13. Inhibition of *E. coli* cell growth by expressing *vp1843* or its mutant genes.

E. coli cells harboring the pBAD/Myc-HisA plasmid containing the *vp1843* gene were cultured at 37°C in the presence of 0.2% glucose (upper panel) or 0.2% arabinose (lower panel), and the cell growth was monitored at absorbance of 590 nm.

inhibited the *E. coli* growth, suggesting that Lys37 and Pro45 in Vp1843 play an essential role in the toxicity toward *E. coli* cells (Hino et al., 2014). Therefore, mutant genes encoding K37N, P45L and K37N/P45L, in which Lys37 and Pro45 in Vp1843 were individually and simultaneously replaced by the corresponding residues Asn and Leu in Vp1830 respectively, were prepared and their influence on the *E. coli* growth in the presence of 0.2% arabinose was tested. As shown in Fig. 2-13, P45L or K37N/P45L expression had little influence on the cell growth, although the K37N expression slightly reduced the cell growth as compared with that of *E. coli* cells with the plasmid vector. This result demonstrated the crucial role of Lys37 and Pro45 in Vp1843 toxicity and suggested that the latter is more essential for the toxicity than the former. Consequently, K37N, P45L, and K37N/P45L were purified as described in materials

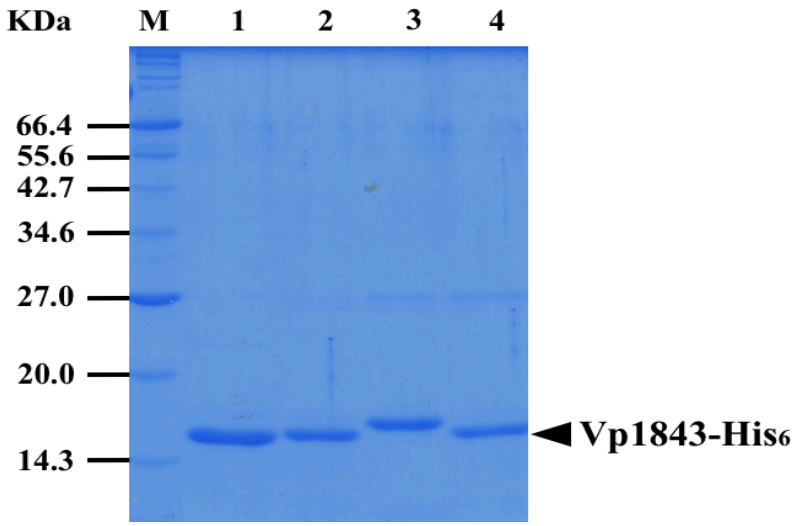

Figure. 2-14. Purification of Vp1843 mutants.

Toxins were purified as described in Materials and Methods and were analyzed by 15% SDS-PAGE. Lane 1, Vp1843-K37N/P45L-His_6; lane 2, Vp1843-P45L-His_6; lane 3, Vp1843-K37N-His_6; lane 4, Vp1843-WT-His_6. M stands for protein molecular weight marker: bovine serum albumin (66.4 KDa), Glutamic dehydrogenase bovine liver (55.6 KDa), maltose-binding protein from *E. coli* (42.7 KDa), thioredoxin reductase from *E. coli* (34.6 KDa), triosephosphate isomerase from *E. coli* (27.0 KDa), trypsin inhibitor from soybean (20.0 KDa), lysozyme from chiken egg white (14.3 KDa).

and methods (Fig. 2-14). The enzymatic potency of K37N, P45L, and K37N/P45L was examined using supercoiled pBR322 as a substrate. The two mutants exhibited little DNA nicking activity toward the supercoiled DNA, as shown in Fig. 2-15, demonstrating that Lys37 and Pro45 in Vp1843 play a crucial role in DNA nicking activity. This result further supported that the DNA nicking activity of Vp1843 is responsible for its high toxicity in *E. coli* cells.

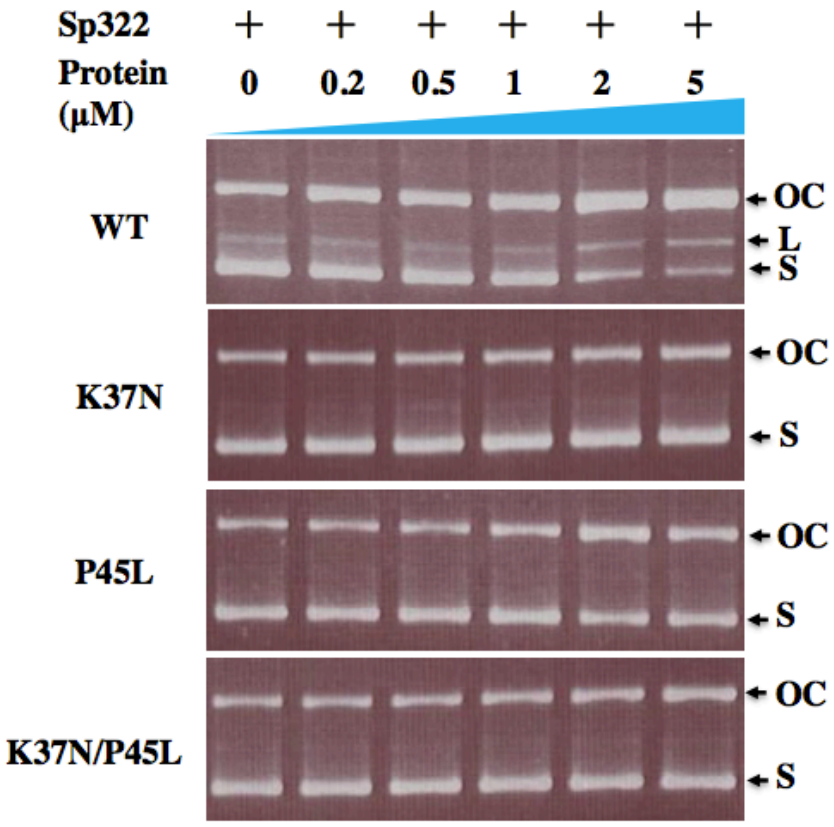

Fig. 2-15. Nicking endonuclease activity of Vp1843 mutants K37N, P45L and K37N/P45L.

Supercoiled pBR322 (100 ng) was incubated with either WT, K37N, P45L, or K37N/P45L of Vp1843 in the nicking reaction buffer. After incubating the reactions at 37°C for 1 h, the DNA products were analyzed in the same manner as described in Materials and Methods. Sp, supercoiled pBR322; OC, L and S indicate open-circular, linear and supercoiled DNA, respectively.

2-4. Summary

The TA system *vp1842/vp1843* found in *V. parahaemolyticus*, has sequence homology to that encoding the *E. coli* TA protein, DinJ/YafQ, However, the toxin Vp1843, unlike its *E. coli* homologue YafQ, has neither protein synthesis inhibitory activity nor ribonuclease activity. Rather, the expression of *vp1843* in *E. coli* resulted in a morphological change in the cells, which could not be seen in the cell expression of YafQ, indicating that Vp1843 has a distinctive activity with that of YafQ.

Meanwhile, we found that Vp1843 has sequence homology not only to *E. coli* YafQ, but also to *C. crescentus* ParE (Fig. 1-7) (Dalton et al., 2010). Phylogenetic studies showed that YafQ and ParE belong to the RelE/ParE superfamily (Fig. 1-8). Toxins belonging to this family share a low similarity in their primary structures, but fold into a similar fold, despite the fact that they display distinct biochemical activities. YafQ is a representative of RelE toxins, performing as a mRNA interferase, while ParE from *Caulobacter crescentus* stands for the ParE toxins, poisoning towards Gyr.

I investigated the inhibition activity of Vp1843 towards Gyr and I found that Vp1843, unlike ParE toxins, exhibits a nicking endonuclease activity. Further characterization on the nicking endonuclease activity of Vp1843 showed that a divalent metal ion is essential for the nicking activity of Vp1843, and the ion preference for Vp1843 is in the order of $Mn^{2+} > Mg^{2+} > Ca^{2+}$. It was also proved that the antitoxin Vp1842 is able to block the nicking activity of Vp1843. I found further that Vp1843 exhibits its nicking activity with an optimum temperature at 25 ~ 50°C and an optimum pH at 7.0 ~ 8.5. Mutations of Lys37 and Pro45 in Vp1843 abolished its nicking activity, suggesting that they play a crucial role in the nicking endonuclease activity.

Chapter 3

Involvement of Vp1842/Vp1843 in the VBNC state

3-1. Introduction

V. parahaemolyticus, a seafood enteropathogen in coastal countries, causes acute gastroenteritis in humans (Nair et al., 2007). A characteristic feature of *V. parahaemolyticus* is that it can become nonculturable at a low temperature in a minimum medium while maintaining at least some metabolic activity, but can be recovered by a temperature up-shift treatment (Kaneko and Colwell., 1975). This phenomenon is termed 'viable but not culturable' (VBNC). Since Colwell and coworkers first reported on the VBNC state (Xu et al., 1982), this phenomenon has now been described for over 50 bacterial species using various criteria for viability and discussed in relation to dormancy and persistency (Oliver et al., 2010). Although the VBNC state has been believed to be a survival strategy in response to certain harsh environmental stresses, no specific factors have been identified because many environmental conditions induce the VBNC state in different bacterial species. Recently, there is a growing evidence that activation of TA systems is one of the mechanisms known to trigger such a state with low metabolic activity (Hayes et al., 2009; Ayrapetyan et al., 2015).

In the previous study (Hino et al., 2014), we found that the *vp1843* expression exhibited severe toxic to *E. coli* cells. In order to examine if the TA system *vp1842/vp1843* is involved in the induction of VBNC state in *V. parahaemolyticus*, I constructed a *vp1842/vp1843* deficient strain (Δ*vp1842/vp1843*) by homologous recombination using a suicide vector pYAK1 and investigated if it could still enter into the VBNC state. A gene map of the suicide vector pYAK1 is shown in Fig. 3-1.

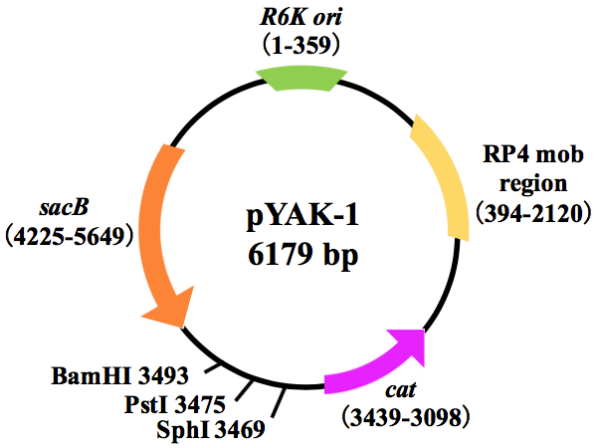

Fig.3-1. A gene map of pYAK1.

The suicide vector pYAK-1 contains a counter-selection marker *sacB* gene, a selection marker *cat* gene, a multiple cloning site, a mob region of the RP4 plasmid and an R6K ori region from plasmid R6K. The *sacB* gene encodes levane saccharase that converts sucrose to levans, which is harmful to bacteria (Reyrat et al., 1998). The *cat* gene encodes chloramphenicol acetyltransferase and confers chloramphenicol resistance. The *R6K ori* initiates replication of the plasmid in *pir* strains, while not in *V. parahaemolyticus*. The mob region mediates transformation of this plasmid to host cells.

3-2. Materials and Methods

3-2-1. Stains

E. coli strain BW19851(F-, *RP4-2(Km:Tn7,Tc::Mu-1), ΔuidA3::pir+, recA1, endA1, thiE1, hsdR17,* creC510) was used to amplify the suicide vector pYAK1. pYAK1 is a R6K origin plasmid, which cannot self-replicate in the absence of π, a functional protein encoded by the *pir* gene (Kolter et al., 1978). Here, *E. coli* stain BW19851 provides π protein for the replication of pYAK1. *V. parahaemolyticus* O3:K6 (TDH+、RIMD2210633) wild-type was used to construct a *vp1842/vp1843* deficient strain.

3-2-2. Plasmids

The suicide vector pYAK1 was kindly provided by Prof. M. Ito and Associate Prof. N. Okino (Kyushu University).

3-2-3. Mediums and reagents

E. coli BW19851 was cultured in LB medium (1% peptone, 0.5% Yeast Extract, 1% NaCl, with or without 20 mg/ml chloramphenicol). *V. parahaemolyticus* was cultured in NB medium (1% peptone, 0.5% Yeast Extract, 3% NaCl). *V. parahaemolyticus* cells completed homologous recombination were screened by TCBS medium (EIKEN CHEMICAL, Japan).

3-2-4. Construction of the suicide vector pYAK-Δ*vp1842/vp1843*-flanking

This was done by two-steps of PCR. First, the DNA fragment of *vp1842/vp1843* with 856 bp upstream and 635 bp downstream flanking sequences was amplified from the genome DNA of wild type *V. parahaemolyticus* with Phusion Hot Start Flex DNA Polymerase (New England Biolabs) using primers upstream-1842-BamHI-F and 1843-downstream-SphI-R (Table 3-1). After treating by BamHI and SphI, the resultant was

ligated into the suicide vector pYAK1 (Fig. 3-2), and pYAK-*vp1842/vp1843*-flanking was used for transformation of *E. coli* BW19851 strain.

Table 3-1. Oligonucleotide used in this study.

Oligonucleotide	Sequence (5'-3')
upstream-1842-BamHI-F	5'-TGCGGATCCGTCTTAAAGCGTTTGTTAGG-3'
1843-downstream-SphI-R	5'-GCAGCATGCTTCAATTGAAGTTCTCAGAAA CAAGTC -3'
Δ184243-Primer-F	5'-CTCAAAGCΔCGTGTACAACACCAGAAACAA AAATTCCC-3'
Δ184243-primer-R	5'-GTACACGGCTTTGAGATGGGCAACTAACAA ACAATTTAAGAG-3'

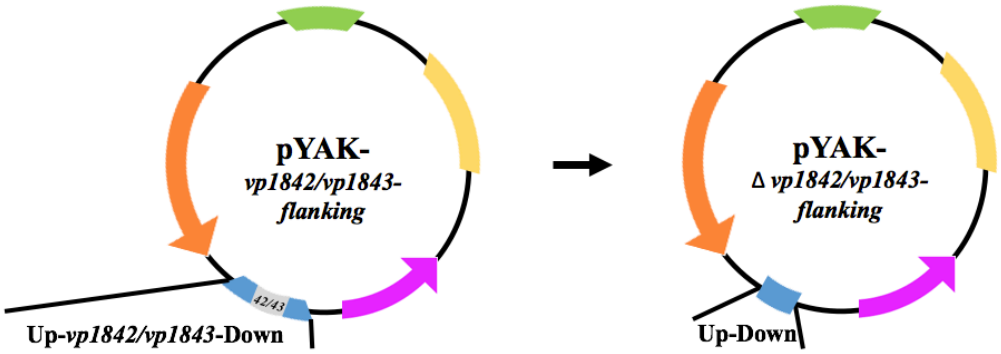

Fig. 3-2. Construction of the suicide vector pYAK-Δ*vp1842/vp1843*-flanking.

The DNA fragment of *vp1842/vp1843* with 856 bp upstream and 635 bp downstream flanking sequences was amplified and ligated into the suicide vector pYAK1 as described in Materials and Methods. The confirmed plasmid pYAK1-*vp1842/vp1843-flanking* was used as a template for the second PCR to delete *vp1842/vp1843*, resulting in a plasmid of pYAK1-Δ*vp1842/vp1843*-flanking. Up and Down indicate upstream and downstream flanking sequences, respectively.

Colonies grown on LB plate with chloramphenicol (20 μg/ml) were further selected by colony PCR with GoTaq Green Master Mix (Promega). The confirmed plasmid

pYAK1-*vp1842/vp1843-flanking* was amplified, extracted, and used as a template for the second PCR. Primers Δ184243-Primer-F and Δ184243-primer-R were used to delete the *vp1842/vp1843* genes from this plasmid by PrimerSTAR Mutagenesis Basal Kit (TaKaRa), resulting in the plasmid of pYAK1-Δ*vp1842/vp1843*-flanking (Fig. 3-2). The construction was confirmed by colony PCR and DNA sequencing and the succeeded suicide vector with only the flanking sequences of *vp1842/vp1843* was used in the following conjugation experiment.

3-2-5. Knockout of the *vp1842/vp1843* genes using homologous recombination

Knockout of the *vp1842/vp1843* gene cluster was carried out by the allelic exchange procedure, as shown in Fig. 3-3. The experiment was carried out as reported previously (Whitaker, et al., 2014). A single colony of *E. coli* stain BW19851 harboring the suicide vector pYAK-Δ*vp1842/vp1843*-flanking and a single colony of wild type *V. parahaemolyticus* (RIMD 2210633) were individually grown in a suitable medium (LB with or without chloramphenicol) at 37°C for 14-16 h. Then, the cells centrifuged at 3,500 g for 5 min were re-suspended in 100 µl LB and mixed well. The mixtures were transferred to a 0.2 µm sterile nitrocellulose membrane filter (Toyo Roshi Kaisha, Japan) located on the surface of an LB plate without antibiotics and incubated at 25°C overnight. The cells were transferred from the membrane to 5 ml LB medium containing 20 µg/ml chloramphenicol and keep at 25°C for 2 h. Then, the cells were spread onto a TCBS (EIKEN CHEMICAL, Japan) plate with 20 µg/mL chloramphenicol and incubated at 25°C overnight. Several colonies were selected, streaked on a TCBS plate containing 10% sucrose and incubated at 37°C for 5 h. For each ancestor cell, 3 colonies of subsequent generations were selected and streaked onto a novel TCBS plate containing 10% sucrose. The knockout of the *vp1842/vp1843* gene cluster in the anticipated cells, Δ*vp1842/vp1843*, was confirmed by colony PCR as well as by DNA sequencing.

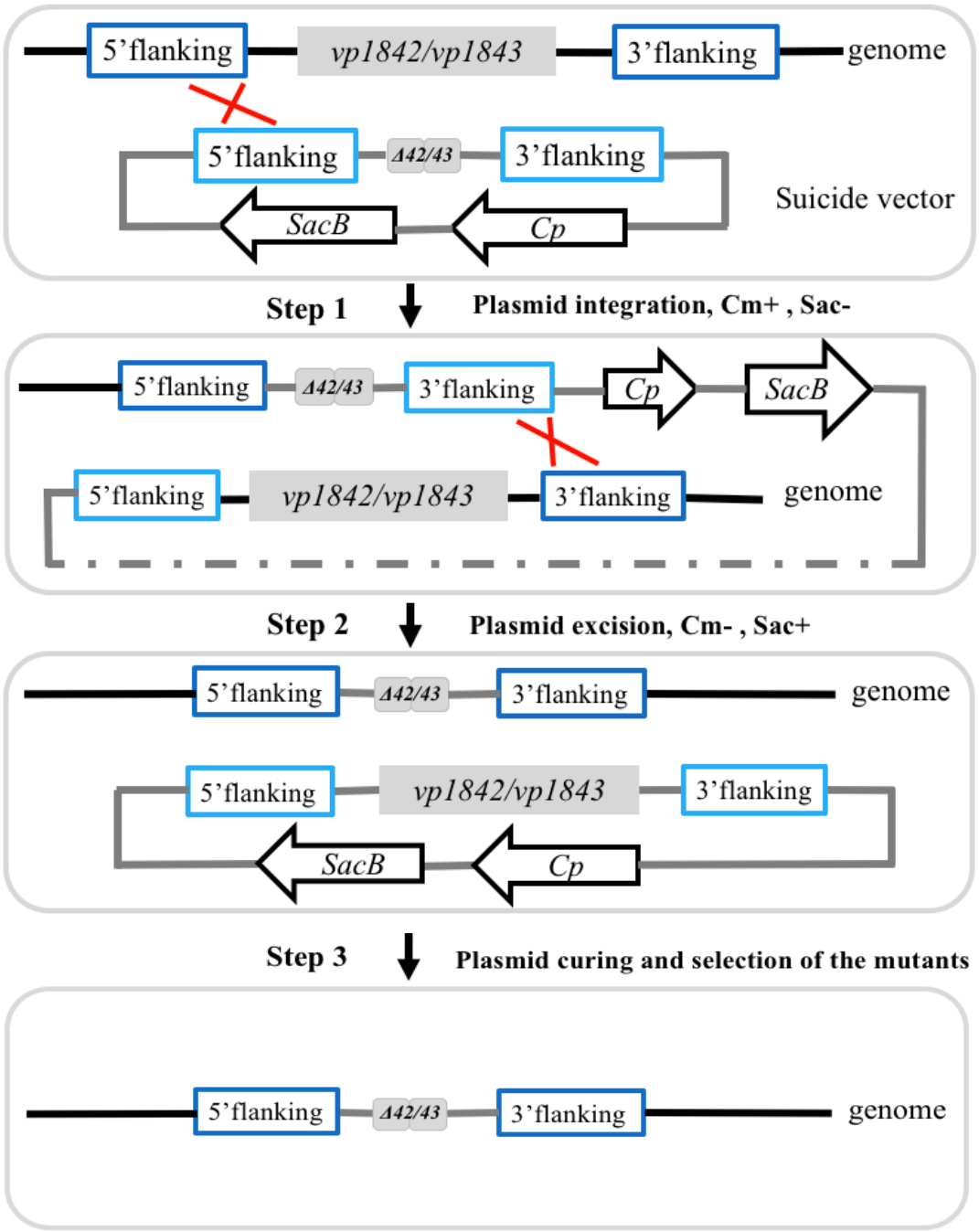

Fig. 3-3. Allelic exchange procedure and Vp-Δvp1842/vp1843 construction.

Step 1: The plasmid pYAK1-Δ*vp1842/vp1843* integrated into the genome of *V. parahaemolyticus,* and the intermediate strain was selected by TCBS medium with 20 μg/ml chloramphenicol. Step 2: Plasmid excised with gene cluster *vp1842/vp1843* and the deficient strain were selected by TCBS with 10% sucrose. Step 3: Plasmid removal happened due to the inability of replication in *V. parahaemolyticus*. Colony PCR was utilized to select the deficient strain.

3-2-6. Induction into the VBNC state

Induction of *V. parahaemolyticus* wild-type or its mutant Δ*vp1842/vp1843* into the VBNC state was carried out as described previously (Hino et al., 2014) with some modifications. The cells were cultured individually in NB medium (EIKEN CHEMICAL, Japan) containing 3% NaCl at 37°C until 0.3 of OD_{660}. The cells were gently harvested with 5,000 rpm for 15 min and washed 3 times with 1.85% NaCl. The cells were re-suspended in 1.85% NaCl, and the starting number of cells was adjusted to 1 x 10^6 CFU/ml. The cells were then incubated at 10°C without shaking for 15 days. Numbers of total cells, viable cells, and culturable cells were counted every day with a Live/Dead BacLight Bacterial Viability Kit L-7007 (Molecular Probes, Waltham, MA) and viewed by fluorescence microscopy. Viable cells with intact membranes were stained green by the fluorescent SYTO 9, while dead cells with compromised membranes were stained red by propidium iodide.

3-2-7. Transcriptome analysis

Total RNA was extracted from *V. parahaemolyticus* in both the normal state and the VBNC state using RNeasy Mini Kit (QIAGEN) and precipitated by 100% ethanol. Then, the RNAs (20μg/100μl) were subjected to next generation sequencing (Macrogen). Functional annotation analysis of the results was performed using DAVID (http://david.abcc.ncifcrf.gov/) based on Gene Ontology (http://geneontology.org/), KEGG (http://www.genome.jp/kegg/) and other functional annotation databases.

3-3. Results

3-3-1. Knock out of *vp1842/vp1843* genes from the *V. parahaemolyticus* genome by conjugation.

Previous studies proved that *V. parahaemolyticus* cells cultured in 1.85% NaCl at 4°C could enter into the VBNC state within two weeks (Hino et al., 2014). In order to investigate whether the TA system *vp1842/vp1843* is involved in the induction into the

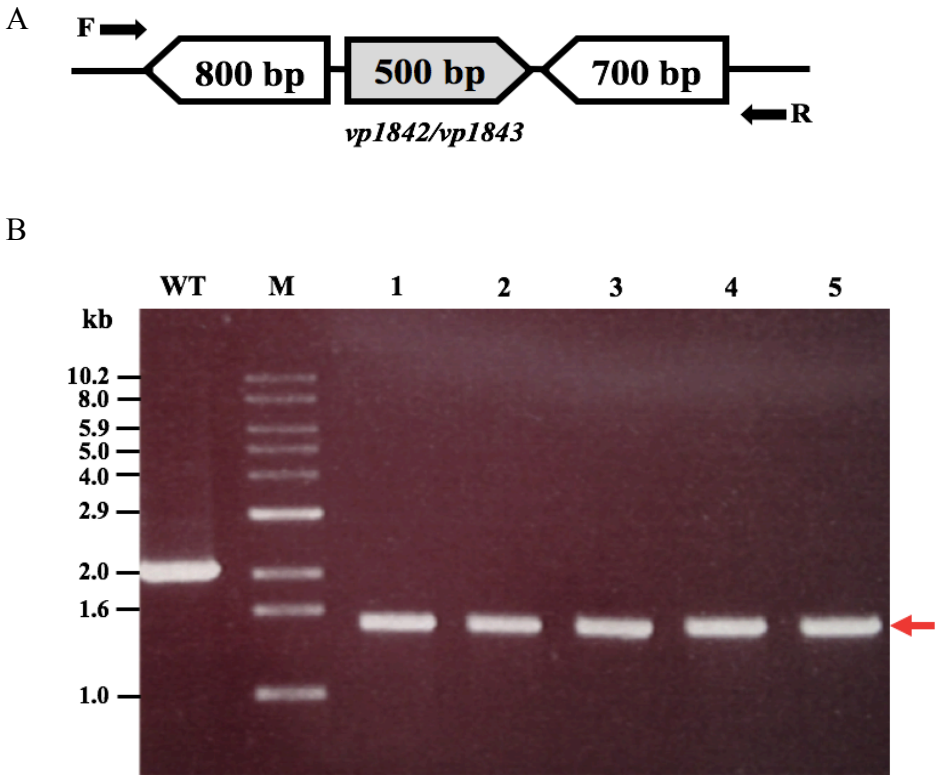

Fig. 3-3. Preparation of the V. parahaemolyticus strain Δvp1842/vp1843.

A; Gene organization neighboring the *vp1842/vp1843* gene in *V. parahaemolyticus* is schematically presented. The genes encoding Vp1842 and Vp1843 are shown in dark grey and flanking genes are in white boxes. F and R primer sets indicated by black arrows were designed in the 5' and 3' flanking regions of *vp1843* and *vp1842* genes, respectively. B; PCR analysis of the gene encoding Vp1843 and Vp1842 confirming deletion of the gene segments in five Δ*vp1842/vp1843* strains (lanes 1-5). DNA size markers were run in lane M.

VBNC state, I knocked out *vp1842/vp1843* from the *V. parahaemolyticus* genome using homologous recombination as described in Materials and Methods. As a result, five transformants termed Δ*vp1842/vp1843* strains were obtained, and they were evaluated by PCR using primer sets designed to amplify the target gene segment with the 5' and 3' flanking regions, as shown in Fig. 3-3. The PCR amplification of each disruptive clone gave DNA products with predicted sizes around 1,500 bp, corresponding to the lengths of flanking genes (Fig. 3-3). In contrast, the genomic DNA from the parent strain indicated amplification of the expected length of the PCR product, corresponding to the sizes of *vp1842/vp1843* and additional flanking regions, as shown in Fig. 3-3. However, when five clones were further cultivated, the clone 5 only gave a single band corresponding to 1,500 bp, while other four clones provided several DNA bands by colony PCR (Data not shown). This finding demonstrated that homologous recombination occurred at the target *vp1842/vp1843* gene in the *V. parahaemolyticus* strain 5 (Δ*vp1842/vp1843*).

3-3-2. Involvement of *vp1842/vp1843* in the VBNC state of *V. parahaemolyticus*

After I obtained the colony (strain5: Δ*vp1842/vp1843*) with *vp1842/vp1843* deficient, I tested to see if it could still enter the VBNC state. The cells were cultured individually in NB medium (EIKEN CHEMICAL, Japan) containing 3% NaCl at 37°C until 0.3 of OD_{660}. The cells were gently harvested after 5,000 rpm for 15 min and washed 3 times with 1.85% NaCl. The cells were re-suspended in 1.85% NaCl, and the starting number of cells was adjusted to 1 x 10^6 CFU/ml. The cells were incubated at 10°C without shaking for 15 days. Numbers of total cells, viable cells, and culturable cells were counted every day with a Live/Dead BacLight Bacterial Viability Kit L-7007 (Molecular Probes, Waltham, MA) and viewed by fluorescence microscopy. Viable cells with intact membranes were stained green by the fluorescent SYTO 9, while dead cells with compromised membranes were stained red by propidium iodide. As shown in Fig. 3-4, the Δ*vp1842/vp1843* mutant, like wild-type *V. parahaemolyticus*, entered

into the VBNC state under stress conditions at a comparable rate with that of the wild-type. Although it is premature on the basis of only a single deletion mutant to draw firm conclusions, this result suggested that the TA system *vp1842/vp1843* is not involved in the VBNC state in *V. parahaemolyticus*. Alternatively, *vp1842/vp1843* may be synergistically involved in the VBNC state with other TA systems in *V. parahaemolyticus*.

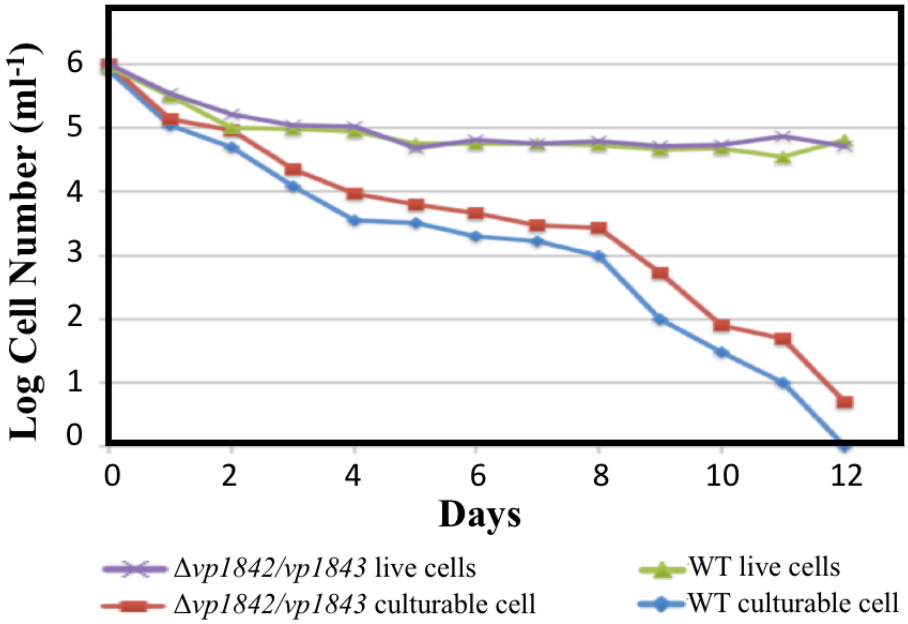

Fig. 3-4. Involvement of the TA system *vp1842/vp1843* in the VBNC state.

Induction of *V. parahaemolyticus* wild-type or its mutant Δ*vp1842/vp1843* into the VBNC state was carried out as described previously (Hino et al., 2014) with some modifications.

3-3-3. Expression level of *vp1842/vp1843* in the VBNC state

The knock-out experiment suggested that the TA system *vp1842/vp1843* is not involved in induction into the VBNC state. In order to confirm this assumption, I compared an expression level of *vp1842/vp1843* in the VBNC state with that in normal growth condition by transcriptome analysis using next-generation sequencer. The result showed that the amounts of transcripts for *vp1842/vp1843* and

vp1829/vp1830 in the VBNC state were comparable to those in normal growth conditions (Table 3-2). This result further supported that *vp1842/vp1843* is not responsible for the VBNC state. Interesting, the deep sequencing analysis showed that the transcript of another TA system *vp1821/vp1820* which is a homolog of *E. coli* TA system *yefM/yoeB* located within SI in the *V. parahaemolyticus* chromosome I increased by 4-folds as compared with that in the normal growth conditions, suggesting its involvement in the VBNC state. Further studies will be required for definition of its implication in the VBNC state.

Table 3-2. Expression level of possible TA systems in the VBNC state and normal state

Gene ID	b/a.fc	N_a	N_b	Homologues in *E. coli*	Identity of Proteins
vp1842	-1.235	6.776	6.471	*dinJ*	22%
vp1843	1.295	6.536	6.910	*yafQ*	17%
vp1829	-1.436	5.207	4.685	*dinJ*	23%
vp1830	1.034	4.462	4.511	*yafQ*	18%
vp1821	4.052	7.634	9.652	*yefM*	45%
vp1820	4.229	7.383	9.463	*yoeB*	63%

- a and b stand for the normal state and the VBNC state, respectively.
- b/a.fc means fold change between two samples using normalized value. A positive value means that the gene in sample b is up-regulated and a negative value means that it is down-regulated. fc=2^(N_b/N_a).
- N stands for normalized value of gene expression by Quantile Normalization.

3-4. Summary

I knocked out the TA system *vp1842/vp1843* from the *V. parahaemolyticus* genome and examined if the mutant (Δ*vp1842/vp1843*) could enter into the VBNC state. The result showed that *vp1842/vp1843* deficient strain-Δ*vp1842/vp1843*, like the wild type *V. parahaemolyticus,* still be able to enter into the VBNC state. This result suggested that *vp1842/vp1843* is not involved in the induction of the VBNC state. To confirm this assumption and also to find genes responsible for the VBNC state, a trancriptome analysis using next-generation sequencer was performed. The result showed that the *vp1842/vp1843* transcript was not up-regulated in the VBNC state. But I found that another TA system *vp1821/vp1820*, which encodes homologues of YefM and YoeB in *E. coli,* showed 4-fold increase in the VBNC state. The involvement of Vp1820 in *V. parahaemolyticus* will be further examined in the future. Further studies will be required to define molecules involved in the VBNC state in *V. parahaemolytics.*

Chapter 4

Physiological function of Vp1843

4-1. Introduction

The type II toxins inhibit cell growth by interfering with vital cellular functions, including DNA replication, protein synthesis, cell-wall biosynthesis, and ATP synthesis (Pandey et al., 2005; Shao et al., 2011). In our pervious study (Hino et al., 2014), I found that Vp1843, unlike RelE/ParE superfamily toxins, has neither protein synthesis inhibitory activity nor Gyr inhibitory activity, rather it has DNA nicking endonuclease activity in this study (Zhang et al., 2017).

As I described in the previous Chapter 3, I found that *vp1842/vp1843* is not involved in the induction into the VBNC state. To investigate physiological functions of *vp1842/vp1843* in *V. parahaemolyticus*, I tried to construct a deletion mutant of the *vp1842* gene and an ectopic expression of the *vp1843* gene in *V. parahaemolyticus*. However, these attempts were unsuccessful, suggesting extreme toxicity of *vp1843* expression in the cells. Our previous study also showed that the expression of *vp1843* in *E. coli* cells caused morphological changes in the cells (Hino et al., 2014). To gain more information about physiological functions of *vp1842/vp1843*, phenotypic properties of *E. coli* cells LMG194 expressing *vp1843* were characterized using fluorescent microscopy and flow cytometry.

4-2. Materials and Methods

4-2-1. Stains

E. coli strain LMG194 (F^- Δ*lac*X74 *gal* E *thi rps*L Δ*pho*A (*Pvu* II) Δ*ara*714 *leu*: Tn*10*) purchased from Invitrogen was used to amplify plasmids harboring *vp1843* and also to express *vp1843* in a well-controlled station. This strain ensures low basal level expression of toxic genes (Guzman et al., 1995). Glucose was used to further suppress the expression of the toxin gene *vp1843* and arabinose was used to promote the *vp1843* expression.

4-2-2. Plasmids

pBAD-Myc-HisA was purchased from Invitrogen and pBAD-Myc-HisA-*vp1843* was a gift from Dr. Hino (Hino et al., 2014).

4-2-3. Mediums and reagents

10 X M9 salts was prepared (for 1 liter) by dissolving 60 g Na_2HPO_4, 30 g KH_2PO_4, 5 g NaCl and 10 g NH_4Cl in MQ and adjusting pH to 7.4 with 10 M NaOH. This was autoclaved for 20 min and stored at room temperature. Casamino acids (2%) was autoclave-sterilized as described above and stored at room temperature. Thiamine(1M), $MgCl_2$ (1 M), glucose (20%) and arabinose (20%) were prepared by filter-sterilize, and stored at -20°C. RMG medium contained 1 X M9 salts, 2% Casamino Acids, 0.2% glucose, 1 mM $MgCl_2$, 50-100 μg/ml ampicillin and 1 mM thiamine. RMA medium was the same as RMG, except that 0.2% glucose was replaced by 0.2% arabinose.

4-2-4. Flow cytometry

E. coli cells containing pBAD/Myc-HisA or pBAD/Myc-HisA with *vp1843* were incubated at 1 x 10^6 cells/mL in RMG medium containing 0.2% glucose and incubated at 30°C, and when the culture reached 1 x 10^8/mL, the exponentially growing culture in a phase of balanced growth was used for further analyses. Measuring the copy

number of the chromosomal DNA was analyzed by the run-off replication method according to (Adachi et al., 2008). Namely, aliquots of exponentially growing cells at 30°C were incubated with rifampicin (300 μg/mL) plus cephalexin (10 μg/mL) for further 3 ~ 4 h at 30°C. Rifampicin inhibits initiation of chromosomal replication, but allows completion of on-going rounds of chromosomal replication. Cephalexin inhibits cell division. After the treatment with the drugs the cells were fixed with 10-fold 80% methanol and kept at 4°C. Before analysis, a small sample of the fixed cells was collected by low-speed centrifugation and suspended in a small volume of water. A solution of 10 μM SYTOX Green Nucleic Acid Stain (Molecular Probes, Inc., Eugene, OR) in DEMSO was added to the cell suspension at a final concentration of 1 μM and kept for 1 h in a dark place. Intensity of fluorescence per cell was measured by flow cytometry, FACS, Calibur (Becton Dickinson Biosciences, K.K., Tokyo, Japan).

4-2-5. Fluorescence microscopy

Expression of the *vp1843* in *E. coli* strain LMG194 was done as described previously (Hino et al., 2014). In brief, a single colony harboring pBAD/Myc-HisA-*vp1843* was pre-cultured at 30°C in RM medium containing 0.2% D-glucose (RMG) until an OD_{590} of 0.5. Then, the culture was divided into two equal parts; half of the cell was collected and re-suspended in fresh RMG, while the other half was re-suspended in fresh RMA (RM medium with 0.2% L-arabinose). Cells were exponentially grown in RMA medium for 3 h, washed in 0.9% NaCl, spotted on poly-L-lysine-coated slide glass and fixed in methanol. Nuclei were visualized with 1 μg/mL DAPI (4',6-Diamidino-2-Phenylindole, Thermo Fisher). Stained cells were photographed by inverted fluorescent microscopy (Eclipse TE2000-U; Nikon) and a digital camera system (AxioCam HRc) with the use of AxioVision Version 4.7.1 software (Carl Zeiss).

4-2-6. Pulse-field electrophoresis

Intact chromosome DNA was extracted and treated as described previously (Ribot et al., 2001; Yamaichi et al., 2007) with some modifications. Cells containing pBAD-Myc-HisA-*vp1843* grown in both RMG and RMA were collected at 25°C by 5,000 rpm

for 5 min when OD_{660} reaches 0.6~0.7. Then, gently re-suspended cells were adjusted to OD_{660}=1.5 in a buffer containing 10 mM Tris-Cl, pH 7.2, 20 mM NaCl, and 50 mM EDTA. Cell lysis and restriction digestion (*Sfi* I or *Xba* I) were done in low melting-point agarose plugs. Then, 1% low melting-point agarose gels containing treated chromosome DNA were electrophoresed at 14°C for 15 h in 0.5× TBE buffer with a ramped pulse time (1~12 sec) and a voltage of 6 V/cm on the equipment (CHEF Mapper or GenePath; Bio-Rad). The band was stained by ethidium bromide solution (50 μg/mL), and observed under UV illumination.

4-3. Results

4-3-1. Expression of *vp1843* in *E. coli* caused apoptosis-like cell death

Several attempts to construct a deletion of the *vp1842* gene and an ectopic expression of the *vp1843* gene in *V. parahaemolyticus* were unsuccessful, suggesting extreme toxicity of *vp1843* expression in the cells. Our previous study showed that the expression of *vp1843* in *E. coli* cells caused morphological changes in the cells (Hino et al., 2014). To gain more information about physiological functions of *vp1842*/*vp1843*, I analyzed the content of the *E. coli* chromosomal DNA in the presence or absence of the *vp1843* gene in the pBAD vector using fluorescence microscopy. As shown in Fig. 4-1, upon induction of *vp1843*, chromosomal DNA experienced a fast and extreme degradation, particularly as indicated by a red arrow (Fig. 4-1, right).

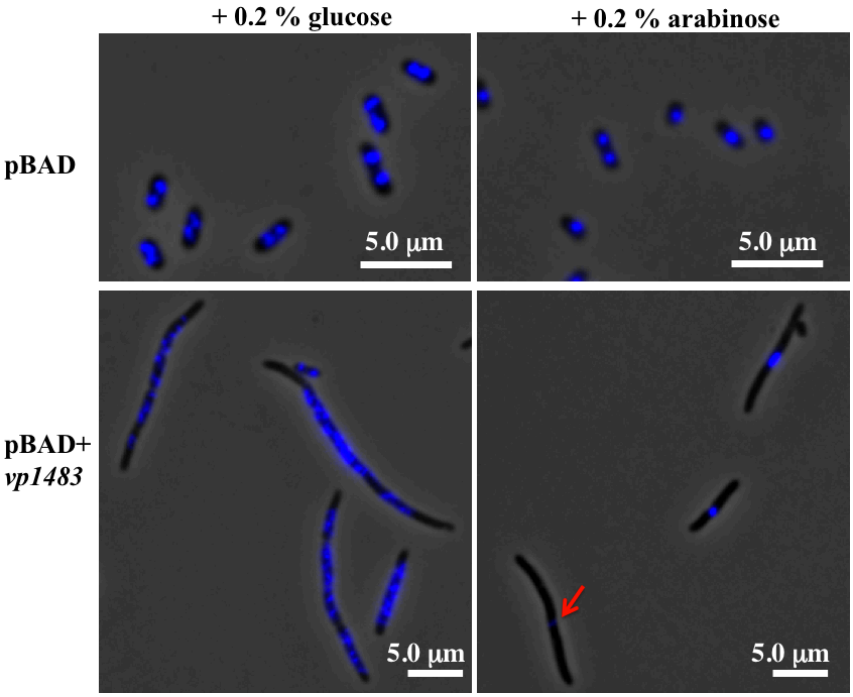

Fig. 4-1. Microscopic analysis of *E. coli* cells repressing or expressing *vp1843*.

E. coli cells containing pBAD/Myc-HisA without *vp1843* (upper lanes) or with *vp1843* (lower lanes) were incubated in the presence of 0.2% glucose or 0.2% arabinose, and the cells were visualized as described in Materials & Methods. The red arrow indicates complete degradation of the *E. coli* chromosomal DNA.

To examine the chromosomal degradation further, I analyzed the content of the *E. coli* chromosomal DNA in the presence or absence of the *vp1843* gene in the pBAD vector using flow cytometry. *E. coli* cells containing pBAD/Myc-HisA or pBAD/Myc-HisA with *vp1843* were incubated at 1 x 10^6 cells/mL in RMG medium containing 0.2% glucose and incubated at 37°C, and when the culture reached 1 x 10^8 cells/mL, the exponentially growing culture in a phase of balanced growth was used for further analyses. Measuring the copy number of the chromosomal DNA was analyzed by the run-off replication method (Adachi et al., 2008). As shown in Fig. 4-2A, the *E. coli* cells containing only the plasmid had the *E. coli* chromosomal DNA, while those harboring pBAD/Myc-HisA containing *vp1843* had a smaller amount of chromosomal DNA, and an additional peak at a position showing a smaller size of chromosomal DNA. This result suggested that a leak expression level of *vp1843* (cultured in RMG medium in the presence of glucose) caused the chromosomal DNA degradation. To corroborate this assumption, the contents of the chromosomal DNA in the *E. coli* cells harboring only the vector plasmid or the plasmid with *vp1843* were compared after 4 h incubation in the presence of rifampicin and cephalexin (Fig. 4-2B). As cephalexin inhibits cell division and rifampicin inhibits replication initiation, but not progress of replisomes, incubation with these drugs allows individual cells to complete the whole chromosome replication. As expected, the *E. coli* cells containing only the vector plasmid contained 4 and 8 copies of the chromosomal DNAs, whereas those harboring the plasmid with *vp1843* had little chromosomal DNA and again an additional peak showing a smaller size of DNA (Fig. 4-2B).

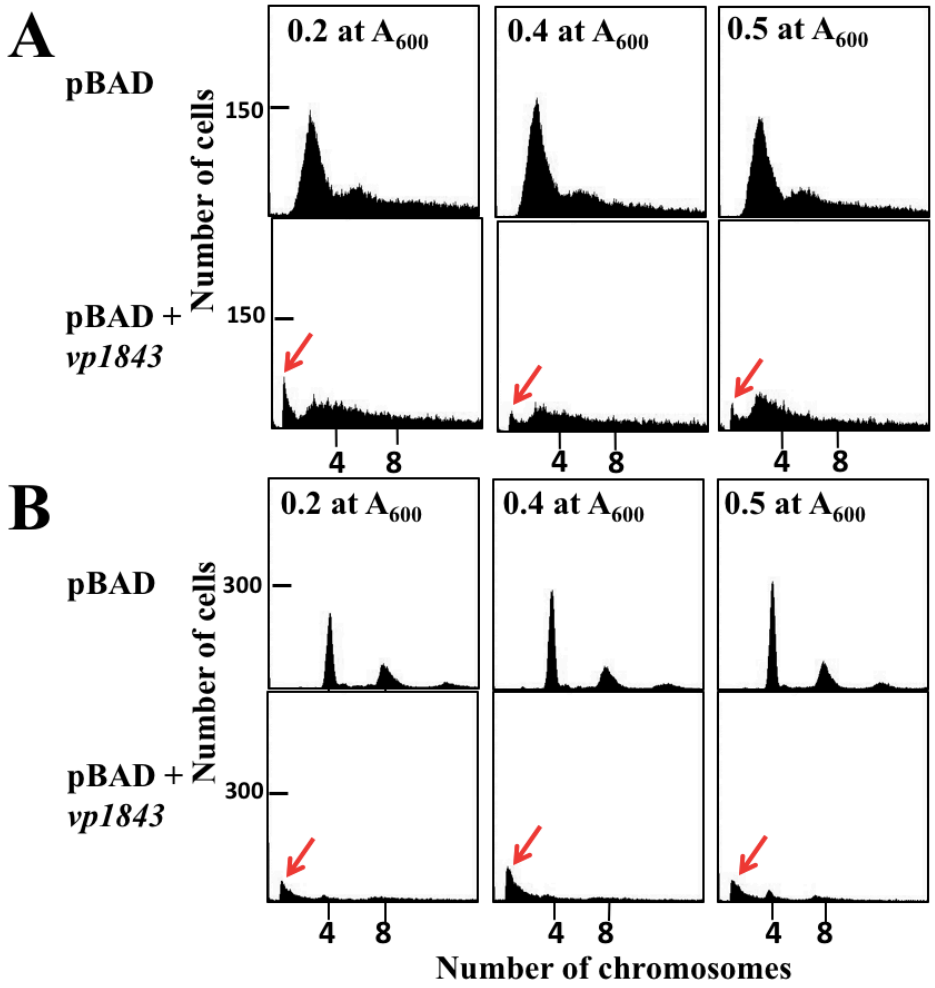

Fig. 4-2. Flow cytometry of *E. coli* cells containing pBAD/Myc-HisA or pBAD/Myc-HisA with *vp1843*.

Flow cytometry of the *E. coli* cells containing pBAD/Myc-HisA (upper panel) or pBAD/Myc-HisA with *vp1843* (lower panel) in the absence (A) or the presence (B) of rifampicin (300 μg/mL) plus cephalexin (10 μg/mL). Arrows indicate additional peaks showing a smaller size of DNA.

To further confirm this assumption, the chromosomal DNA degradation was evaluated by pulse-field electrophoresis (Fig. 4-3). Namely, the chromosomal DNA was isolated from either *E. coli* cells with or without the *vp1843* expression, digested with restriction enzymes *Sfi* I or *Xba* I, and the resulting mixtures were subjected to pulse-field electrophoresis, as described in Materials and Methods. Apparently, the *E. coli* cells grown in RMA had a smaller amount of chromosomal DNA than those grown

in RMG. In addition, the restriction patterns of the chromosomal DNA isolated from *E. coli* cells grown in RMG were slightly distinct from those of the *E. coli* cells grown in RMA, as indicated in Fig. 4-1. This result suggested further that the *vp1843* expression caused DNA degradation throughout the *E. coli* chromosome.

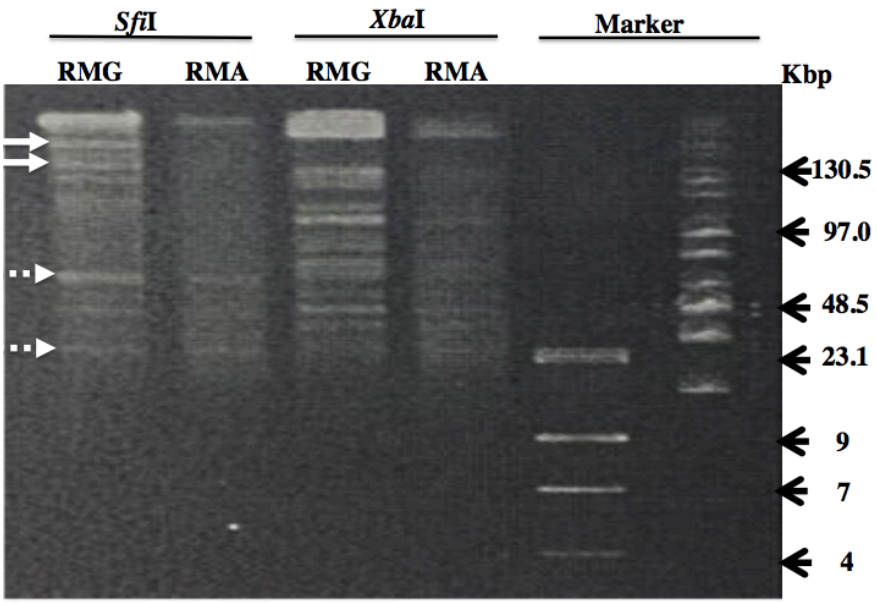

Fig. 4-3. Pulsed-field polyacrylamide electrophoresis.

RMG and RMA indicate the chromosomal DNA extracted from *E. coli* cells grown in RMG and RMA, respectively. Straight and broken white arrows indicate representative DNA fragments visible in the chromosomal DNA from *E. coli* grown in RMG and those visible in both chromosomal DNAs from *E. coli* cells grown in RMG and RMA, respectively.

4-4. Summary

To examine physiological functions of *vp1842*/*vp1843*, I examined effects of the *vp1843* expression on *E. coli* LMG194 cells using pBAD-Myc-HisA. The results showed that *E. coli* cells harboring a pBAD-Myc-HisA-*vp1843* experienced a severe morphological change even in the presence of 0.2% glucose. While upon expression of *vp1843*, a severe DNA degradation was observed. Flow cytometry showed that a smaller amount of chromosomal DNA exists in the cells harboring pBAD-Myc-HisA containing *vp1843* even in the absence of arabinose, suggesting a leak expression of *vp1843* induced the chromosomal DNA degradation. To exclude the possibility that the small amount of DNA was due to DNA replication arrest, a cell division inhibitor cephalexin and a DNA replication initiation factor rifampicin were added to the RMG and RMA medium, and the contents of the chromosomal DNA in the *E. coli* cells harboring only the vector plasmid or the plasmid with vp1843 were compared after 4 h incubation. As expected, the *E. coli* cells containing only the vector plasmid contained 4 and 8 copies of the chromosomal DNAs, whereas those harboring the plasmid with *vp1843* had little chromosomal DNA (Fig. 4-2). Furthermore, the degradation pattern of chromosomal DNA upon *vp1843* expression was compared by pulse-field electrophoresis. The results showed that restriction patterns of the chromosomal DNA isolated from *E. coli* cells grown in RMG were slightly distinct from those of the *E. coli* cells grown in RMA, as indicated in Fig. 4-3. This result suggested further that the *vp1843* expression caused DNA degradation throughout the *E. coli* chromosome.

Chapter 5

General considerations

The type Ⅱ TA systems, being abundant in bacterial and archaeal genomes, are small genetic elements composed of two genes organized on an operon which encodes a stable toxin and a labile cognate antitoxin, respectively. Under unfavorable conditions, such as amino acid poverty and DNA damage, the antitoxin is degraded, leading to the toxin activation, and consequently, the toxin arrests cell growth by its cellular effects, such as ribosome-dependent mRNA cleavage activity (mRNA interferase) or DNA gyrase (Gyr) inhibitory activity. Previously, we found that a gene cluster, *vp1842/vp1843*, within a superintegron on the *V. parahaemolyticus* genome, has homology to that encoding the *E. coli* TA protein, DinJ/YafQ (Hino et al., 2014). However, the toxin Vp1843, unlike the *E. coli* homologue YafQ, has no mRNA interferase activity. During the course of this study, I found that the *V. parahaemolyticus* toxin Vp1843 has DNA nicking endonuclease activity.

A large number of DNA nicking endonucleases have been found in a variety of organisms and were investigated extensively from both structural and functional point of view (Pingoud et al., 2014; Xu, 2015). Some nicking enzymes and engineered nicking enzymes have become invaluable tools in diagnostic probes for cancer cells and in genome modifications (Pingoud et al., 2014; Xu, 2015). These nicking enzymes have been grouped into main three classes, PD-D/EXK, HNH and GIY-YIG, based on the amino acid residues (amino acid motifs) comprised catalytic sites (Pingoud et al., 2014; Xu, 2015). Vp1843 found in this study has no sequence similarity to any known DNA nicking endonucleases; therefore, it is a novel nicking endonuclease. Mutational analysis identified Lys37 and Pro45 in Vp1843 as crucial residues in the DNA nicking activity. We previously constructed a three-dimensional model of Vp1843 using the structure of the *C. crescentus* ParD-ParE as a template in the Swiss-Model Server (Fig. 5-1). In our model, Lys37 is located at α2 and its side chain appears to be exposed in solution, while Pro45 lies between α2 and α3 and appears to interrupt continuous helix

formation of α2. Further biochemical and structural studies of Vp1843 should assign functional implication of these amino acids.

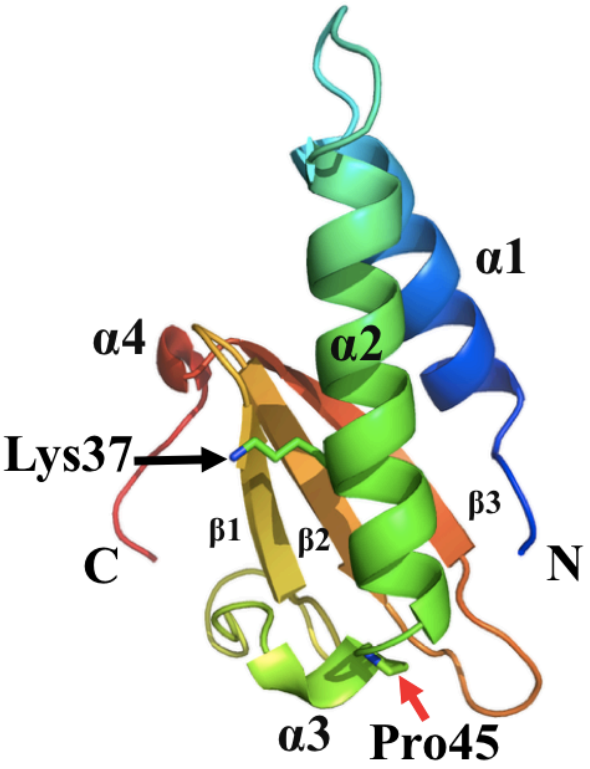

Fig. 5-1. Three-dimensional structures of Vp1843.

Three-dimensional model of Vp1843 was constructed with the Swiss-Model Server (http://swissmodel.expasy.org) using *Caulobacter crescentus* ParE (PDB code 3KXE) as a template (Gupta et al., 2016). The secondary structures are labeled, and N and C termini are indicated. The side chains of essential amino acids Lys37 and Pro45 for the nicking activity are indicated.

Vp1843 belongs to the RelE/ParE superfamily. It is generally accepted that proteins with similar backbone conformations have similar biological activities. This rule therefore seems to be inapplicable to the RelE/ParE superfamily toxins. The RelE/ParE toxins fold into a similar fold, despite the fact that the toxins belonging to this family display two distinct biochemical activities (Francuski and Saenger., 2009). Namely, the RelE family toxins, such as YafQ and YoeB, stall the ribosome by cleaving mRNA in

a translation-dependent fashion (Pedersen, 2003), while the ParE family toxins have been reported to interfere with DNA replication by inhibiting Gyr (Jiang et al., 2002). However, their biological activities are still controversial. The crystal structure of the *E. coli* RelE in complex with the *Thermus thermophilus* ribosome revealed that Arg81 and Tyr87 plays an essential role in mRNA interferase activity as general acid and base, respectively (Neubauer et al., 2009). Furthermore, structural and biochemical studies on YafQ found that His50, His63, Asp67 and His87 participate in acid-base catalysis during mRNA hydrolysis and further suggested that Phe91 plays an important role in mRNA positioning (Maehigashi et al., 2015). Since these catalytic residues in RelE and YafQ are not conserved in the RelE family toxins, it is thus unlikely that the RelE proteins simply catalyze mRNA cleavage by general acid-base catalysis. Griffin *et al* described that RelE may represent a shift in the RNase general acid-base catalytic paradigm and principally promote catalysis via transition-state charge stabilization and leaving group protonation (Griffin et al., 2013).

As for ParE toxins, the molecular basis for inhibitory activity toward Gyr remains unclear. First, RK2 plasmid ParE and *V. cholerae* ParE2 stabilize the cleavage complex by interacting with GyrA, despite having distinct binding sites (Jiang et al., 2002; Yuan et al., 2010). Second, *Mycobacterium turbaclosis* ParE inhibits DNA gyrase by interacting with GyrB, the C-terminal residues being suggested to be involved in the inhibitory activity (Gupta et al., 2016). Third, *E. coli* ParE2 interacts with neither GyrA nor GyrB, although its Gyr inhibitory activity has not been experimentally verified (Sterckx et al., 2016). In the present study, I found that the *V. parahaemolyticus* toxin Vp1843 is a DNA nicking endonuclease. Hence, the present result may assign the DNA nicking endonuclease activity as a third biological activity in the RelE/ParE superfamily toxins (Fig. 5-2). Further study, particularly on ParE toxins, will provide a definite biological activity of the RelE/ParE superfamily toxins.

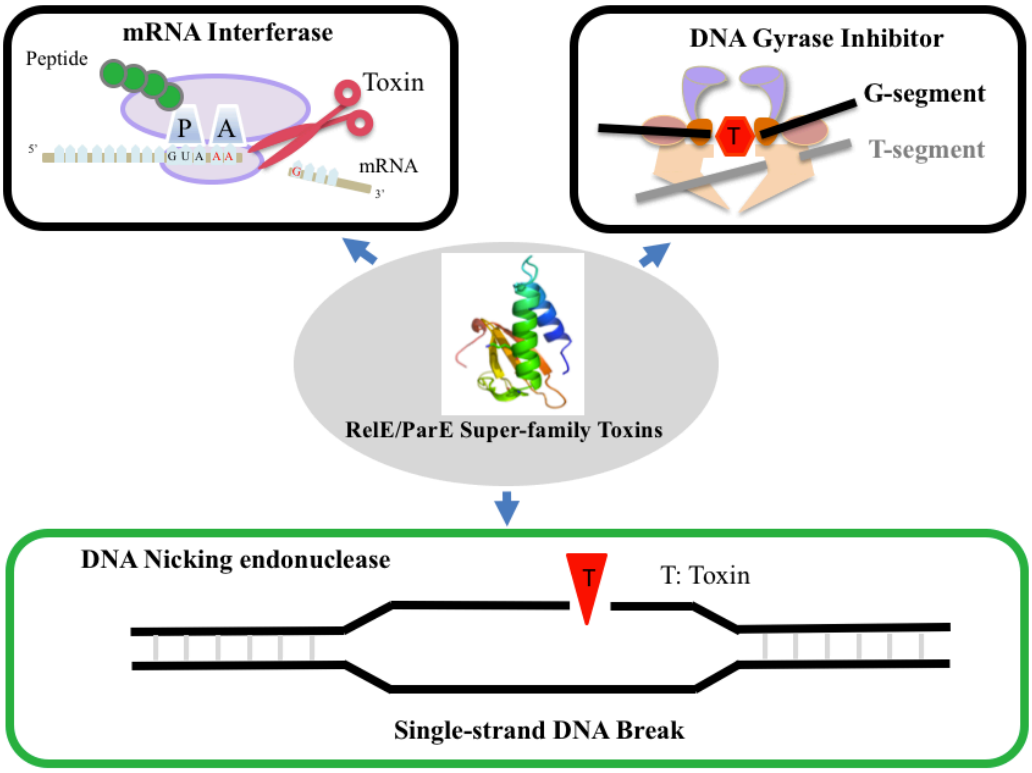

Fig. 5-2. Schematic of functions of toxins belonging to RelE/ParE superfamily.

Toxins which belong to the RelE/ParE superfamily fold into a similar fold, while they display distinct biochemical activities. The RelE toxins, such as YafQ and YoeB, cleave mRNA (mRNA interferase), while the ParE toxins inhibit DNA gyrase. The present study may assign the DNA nicking endonuclease activity as a third biological activity in the RelE/ParE superfamily.

V. parahaemolyticus, a seafood enteropathogen in coastal countries, causes acute gastroenteritis in humans. A characteristic feature of *V. parahaemolyticus* is that it can become viable, but not culturable (VBNC), at a low temperature in a minimum medium. Since Colwell and coworkers first reported on the VBNC state, this phenomenon has now been described for over 50 bacterial species using various criteria for viability and discussed in relation to dormancy and persistency. Yet, the molecular involved in VBNC state induction is still unveil. Recently, there is a

growing evidence that activation of TA systems is one of the mechanisms known to trigger such a state with low metabolic activity in which a possible role of TA systems has been suggested. In order to examine the involvement of *vp1842/vp1843* in the VBNC state, I constructed Δ*vp1842/vp1843*, in which *vp1842/vp1843* was deleted by homologous recombination and tested if Δ*vp1842/vp1843* could enter into the VBNC state. The result suggested *vp1842/vp1843* is not involved in the VBNC state. Alternatively, *vp1842/vp1843* may be synergistically involved in the VBNC state with other TA systems in *V. parahaemolyticus*. To consider these possibilities, I performed the transcriptome analysis in both VBNC state and the normal state. The result showed that the *vp1843* expression was almost same as that in the normal state. However, I found that the transcript for the TA system *vp1821/vp1820* located within SI in the *V. parahaemolyticus* chromosome I showed a four-fold up-regulation in the VBNC state, indicating that it may be involved in VBNC induction. Further experiments are required to decide the molecules induced the VBNC state in *V. parahaemolyticus.*

The *vp1843* expression in *E. coli* cells caused the chromosomal DNA degradation. In bacteria, SOS is a global response to DNA damage, mediated by the recA-lexA genes, resulting in cell cycle arrest, DNA repair, and mutagenesis. However, it has also been described that under severe DNA damage strong activation of RecA occurs, leading to the apoptosis-like death pathway, characterizing DNA fragmentation (Erental et al., 2014). Vp1843 has DNA nicking activity towards DNA. It is thus likely that the *vp1843* expression results in severe DNA damage, leading to DNA degradation and the apoptosis-like death. Interestingly, *vp1842/vp1843* locates in a superintegron in the *V. parahaemolyticus* chromosome I (Makino et al., 2003). The superintegrons, which are genomic islands at least 100 kb in size and contain a large number of open reading frames encoding proteins with no known function, have been discovered in the genomes of diverse proteobacterial species (Rowe-Magnus et al., 2003). They are thought to be massive ancestral versions of multiresistance integrons, in which several

antibiotic-resistant genes are located. It has been reported that when located in genomic islands, TA systems participate in stabilization, which is reminiscent of post-segregational killing mediated by plasmid-encoded TA systems (Hallez et al., 2010). Probably, when the superintegron including *vp1842/vp1843* within the chromosome I is lost or damaged, the activated Vp1843 nicks the chromosomal DNA, which results in severe DNA damage, leading to DNA degradation and the apoptosis-like death (Fig. 5-3). Thus, *vp1842/vp1843* may be involved in the maintenance of the superintegron in the *V. parahaemolyticus* chromosome I in a manner similar to post-segregational killing.

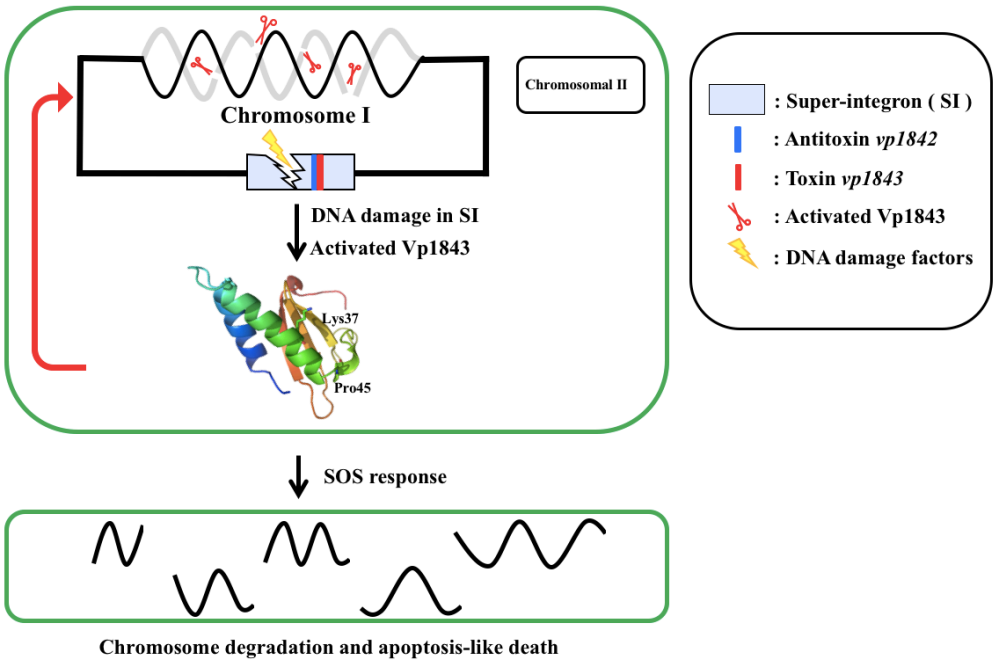

Fig. 5-3. A hypothetical mechanism of Vp1843 in chromosome maintenance.

Based on the genomic location of *vp1843*, the nicking activity of Vp1843 and the chromosome DNA degradation upon *vp1843* expression, I propose that when the SI including *vp1842*/*vp1843* within the chromosome I is lost or damaged, the activated Vp1843 nicks the chromosomal DNA, which results in severe DNA damage, leading to DNA degradation and the apoptosis-like death.

References

Aakre, C.D., Phung, T.N., Huang, D. and Laub, M.T. (2013) A bacterial toxin inhibits DNA replication elongation through a direct interaction with the sliding clamp. Mol. Cell. 52: 617-628.

Aakre, C.D. (2015) Toxin-antitoxin systems in bacteria: targets, mechanisms and specificity. Doctoral thesis.

Adachi, S., Fukushima, T. and Hiraga, S. (2008) Dynamic events of sister chromosomes in the cell cycle of *Escherichia coli*, Genes to Cells. 13: 181-197.

Aizenman, E., Engelberg-Kulka, H. and Glaser G. (1996) An *Escherichia coli* chromosomal 'addiction module' regulated by guanosine 3',5'-bispyrophosphate: a model for programmed bacterial cell death. Proc. Natl. Acad. Sci. USA. 93: 6059-6063.

Ayrapetyan, M., Williams, T.C. and Oliver D. (2015) Bridging the gap between viable but non-culturable and antibiotic persistent bacteria, Trends Microbiol. 23: 7-13.

Bates, T.C and Oliver, J.D. (2004) The viable but nonculturable state of kanagawa positive and negative strains of Vibrio parahaemolyticus. J. Microbiol. 42: 74-79.

Christensen, S.K., Maenhaut-Michel, G., Mine, N., Gottesman, S., Gerdes, K., van Melderen, L., (2004) Overproduction of the Lon protease triggers inhibition of translation in *Escherichia coli*: involvement of the yefM-yoeB toxin-antitoxin system. Mol. Microbiol. 51: 1705-1717.

Christensen, S.K., Mikkelsen, M., Pedersen, K., Gerdes, K. (2001) RelE, a global inhibitor of translation, is activated during nutritional stress. Proc. Natl. Acad. Sci. USA. 98: 14328-14333.

Collin, F., Karkare, S., Maxwell, A. (2011) Exploiting bacterial DNA gyrase as a drug target: current state and perspectives. Appl. Microbiol. Biotechnol. 92: 479-497.

Dalton, K., Crosson, S. (2010) A conserved mode of protein recognition and binding in a ParD-ParE toxin-antitoxin complex. Biochemistry. 49: 2205-2215.

Du, M., Chen, J., Zhang, X., Li, A., Li, Y., Wang, Y. (2007) Retention of virulence in a viable but nonculturable Edwardsiella tarda isolate. Appl. Environ. Microbiol. 73: 1349-1354.

Erental, A., Kalderon, Z., Saada, A., Smith, Y., Engelberg-Kulka, H. (2014) Apoptosis-like death, an extreme SOS response in *Escherichia coli*, mBio. 5: e01426-14.

Fineran, PC., Blower, TR., Foulds, I.J., Humphreys, D.P., Lilley, K.S., Salmond, G.P. (2009) The phage abortive infection system, ToxIN, functions as a protein-RNA toxin-antitoxin pair. Proc. NatI. Acad. Sci. USA. 106: 894-899.

Francuski, D., Saenger, W. (2009) Crystal structure of the antitoxin-toxin protein complex RelB-RelE from Methanococcus jannaschii. J. Mol. Biol. 393: 898-908.

Fujino, T., Okuno, Y., Nakada, D., Aoyama, A., Mukai, T., and Ueho, T. (1953) On the bacteriological examination of shirasu food poisoning. Med. J. Osaka Univ. 4: 299-304.

Gellert, M., Mizuuchi, K., O'Dea, M.H. and Nash, H.A. (1976) DNA gyrase: an enzyme that introduces superhelical turns into DNA. Proc. Natl. Acad. Sci. U.S.A. 73: 3872-3876

Gerdes, K., Bech, F.W., Jorgensen, S.T., Lobner-olesen, A., Rasmussen, P.B., Atlung, T., Boe, L., Karlstrom, O., Molin, S., and von Meyenburg, K. (1986a). Mechanism of postsegregational killing by the hok gene product of the parB system of plasmid R1 and its homology with the relF gene product of the E. coli relB operon. EMBO J. 5: 2023-2029.

Gerdes, K., Rasmussen, P.B., Molin, S., (1986b) Unique type of plasmid maintenance function: postsegregational killing of plasmid-free cells. Proc. Natl. Acad. Sci. USA. 83: 3116-3120.

Griffin, M.A., Davis, J.H., Strobel, S.A. (2013) Bacterial toxin RelE: A highly efficient nuclease with exquisite substrate specificity using atypical catalytic residues. Biochemistry. 52: 8633-8642.

Gupta, M., Nayyar, N., Chawla, M., Sitaraman, R., Bhatnagar, R., Banerjee, N. (2016) The chromosomal parDE2 toxin-antitoxin system of Mycobacterium tuberculosis H37Rv: genetic and functional characterization, Front. Microbiol. 7. Article 886.

Guzman, L.M., Belin, D., Carson, M.J., Beckwith, J. (1995) Tight regulation, modulation, and high- level expression by vectors containing the arabinose PBAD promoter. J Bacteriol. 177: 4121-4130.

Gubaev, A., Weidlich, D., Klostermeier, D. (2016) DNA gyrase with a single catalytic tyrosine can catalyze DNA supercoiling by a nicking-closing mechanism. Nucleic Acids Res. 44: 10354-10366.

Hallez, R., Geeraerts, D., Sterckx, Y., Mine, N., Loris, R., Melderen, L.V. (2010) New toxins homologous to ParE belonging to three-component toxin-antitoxin systems in Escherichia coli O157:H7. Mol. Microbiol. 76: 719-732.

Hayes, C.S. and Low, D.A. (2009) Signals of growth regulation in bacteria. Curr Opin Microbiol. 12: 667-673.

Hino, M. (日野まど香) (2014) 腸炎ビブリオ (*vibrio parahaemolyticus*) の”生きているが培養できない” (VBNC) 状態とその誘導因子に関する研究. Doctoral thesis.

Hino, M., Zhang, J., Takagi, H., Miyoshi, T., Uchiumi, T., Nakashima, T., Kakuta, Y. and Kimura, M. (2014) Characterization of putative toxin/antitoxin systems in *Vibrio parahaemolyticus.* J Appl Microbiol.117:185-195.

Jiang, Y., Pogliano, J., Helinski, D.R., Konieczny, I. (2002) ParE toxin encoded by the broad-host-range plasmid RK2 is an inhibitor of *Escherichia coli* gyrase. Mol Microbiol. 44**:** 971-979.

Kaneko, T., Colwell, R.R. (1975) Incidence of *Vibrio parahaemolyticus* in Chesapeake Bay, Appl. Microbiol. 30: 251-257.

Kolter, R., Inuzuka, M. and Helinski, D.R. (1978). Trans-complementation-dependent replication of a low molecular weight origin fragment from plasmid RK6. Cell. 15:1199-1208.

Lee, K.Y., Lee, K.Y., Kim, J.H., Lee, I.G., Lee, S.H., Sim, D.W., Won, H.S., Lee, B.J. (2015) Structure-based functional identification of *Helicobacter pylori* HP0268 as a nuclease with both DNA nicking and RNase activities. Nucleic Acids Res. 43: 5194-5207.

Letchumann, V., Chan, K.G., L, L.H. (2014) Vibrio parahaemolyticus: a review on the pathogenesis, prevalence, and advance molecular identification techniques. Front Microbiol. 5: 705

Li, L., Mendis, N., Trigui, H., Oliver, J.D and Faucher, P. (2014) The importance of the viable but non-culturable state in human bacterial pathogens. Front Microbiol.5:258.

Maehigashi, T., Ruangprasert, A., Miles, S.J., Dunham, C.M. (2015) Molecular basis of ribosome recognition and mRNA hydrolysis by the *E. coli* YafQ toxin. Nucleic Acids Res. 43: 8002-8012.

Makino, K., Oshima, K., Kurokawa, K., Yokoyama, K., Uda, T., Tagomori, K., Iijima, Y., Najima, M., Nakano, M., Yamashita, A., Kubota, Y., Kimura, S., Yasunaga, T., Honda, T., Shinagawa, H., Hattori, M., Iida, T. (2003) Genome sequence of Vibrio parahaemolyticus: a pathogenic mechanism distinct from that of *V. cholera*, The Lancet 361: 743-749.

Mashimo, C. (真下千穂). (2006). スーパーインテグロン：細菌の耐性獲得における新たな戦略. 日本細菌学雑誌. 61: 339-334.

Masuda, H., Tan, Q., Awano, N., Wu, K.P. and Inouye, M. (2012) YeeU enhances the bundling of cytoskeletal polymers of MreB and FtsZ, antagonizing the CbtA (YeeV) toxicity in *Escherichia coli*. Mol. Microbiol. 84: 979-989.

Masuda, Y., Miyakawa, K., Nishimura, Y., Ohtsubo, E., (1993) chpA and chpB, *Escherichia coli* chromosomal homologs of the pem locus responsible for stable maintenance of plasmid R100. J. Bacteriol. 175: 6850-6856.

McCarter. (1999) The Multiple Identities of Vibrio parahaemolyticus J. Molec. Microbiol. Biotechnol. 1: 51-57.

Nair, G.B., Ramamurthy, T., Bhattacharya, S.K., Dutta, B., Takeda, Y., Sack, D.A. (2007) Global dissemination of *Vibrio parahaemolyticus* serotype 03: K6 and its serovariants, Clin. Microbiol. Rev. 20: 39-48.

Neubauer, C., Gao, Y.G., Andersen, K.R., Dunham, C.M., Kelley, A.C., Hentschel, J., Gerdes, K., Ramakrishnan, V., Brodersen, D.E. (2009) The structural basis for

mRNA recognition and cleavage by the ribosome-dependent endonuclease RelE. Cell.139: 1084-1095.

Ogura, T., Hiraga, S. (1983) Mini-F plasmid genes that couple host cell division to plasmid proliferation. Proc. Natl. Acad. Sci. USA. 80: 4784-4788.

Oliver, J.D. (2010) Recent findings on the viable but nonculturable state in pathogenic bacteria, FEMS Microbiol. Rev. 34: 415-425.

Page, R. and Peti, W. (2016) Toxin-antitoxin systems in bacterial growth arrest and persistence, Nat. Chem. Biol. 12: 208-214.

Pai, S.R., Actor, J.K., Sepulveda, E., Hunter RL-Jr., Jagannath, C. (2000) Identification of viable and non-viable *Mycobacterium tuberculosis* in mouse organs by directed RT-PCR for antigen 85B mRNA. Microb. Pathog. 28: 335-342.

Pandey, D.P., Gerdes, K. (2005) Toxin-antitoxin loci are highly abundant in free-living but lost from host-associated prokaryotes, Nucleic Acids Res. 33: 966-976.

Pedersen, K., Zavialov, A.V., Pavlov, M.Y., Elf, J., Gerdes, K., Ehrenberg, M. (2003) The bacterial toxin RelE displays codon-specific cleavage of mRNAs in the ribosomal a site. Cell. 112: 131-140.

Pingoud, A., Wilson, G.G., Wende, W. (2014) Type II restriction endonuclease—a historical perspective and more. Nucleic Acids Res. 42: 7489-7527.

Reyrat, J.M., Pelicic, V., Gicquel, B., Rappuoli, R. (1998) Counterselectable Markers: Untapped Tools for Bacterial Genetics and Pathogenesis. Infect Immun. 66: 4011-4017.

Ribot, E.M., Fitzgerald, C., Kubota, K., Swaminathan, B., Barrett, T.J. (2001) Rapid Pulsed-Field Gel Electrophoresis Protocol for Subtyping of *Campylobacter jejuni*, J Clin Microbiol. 39: 1889-1894.

Rivers, B., Steck, T.R. (2001) Viable but nonculturable uropathogenic bacteria are present in the mouse urinary tract following urinary tract infection and antibiotic therapy. Urol. Res. 29: 60-66.

Rowe-Magnus, D.A., Guerout, A.M., Biskri, L., Bouige, P., Mazel, D. (2003) Comparative analysis of superintegrons: engineering extensive genetic diversity in the Vibrionaceae, Genome Res. 13: 428-442.

Rowe-Magnus, D.A., Guerout, A.M., Ploncard, P., Dychinco, B., Davies, J., Mazel, D. (2001) The evolutionary history of chromosomal super-integrons provides an ancestry for multiresistant integrons. Proc Natl Acad Sci USA. 98: 652-657.

Sevin, E.W., Barloy-Hubler, F. (2007) RASTA-Bacteria: a web-based tool for identifying toxin-antitoxin loci in prokaryotes. Genome Biol. 8:155.

Shao, Y., Harrison, E.M., Bi, D., Tai, C., He, X., Ou, H.Y., Rajakumar, K., Deng, Z. (2011) TADB: a web-based resource for Type 2 toxin-antitoxin loci in bacteria and archaea, Nucleic Acids Res. 39: 606-611.

Short, F.L., Pei, X.Y., Blower, T.R., Ong, S.L., Fineran, P.C., Luisi, B.F., Salmond, G.P. (2013) Selectivity and self-assembly in the control of a bacterial toxin by an antitoxic noncoding RNA pseudoknot. Proc. NatI. Acad. Sci. USA. 110: 241-249.

Sterckx, Y.G.J., Jove, T., Shkumatov, A.V., Garcia-Pino, A., Geerts, L., Kerpel, M.D., Lah, J., Greve, H.D., Van Melderen, L., Loris, R. (2016) A unique hetero-hexadecameric architecture displayed by the Escherichia coli O157 PaaA2-ParE2 antitoxin-toxin complex. J. Mol. Biol. 428: 1589-1603.

Thisted, T., Gerdes K. (1992) Mechanism of post-segregational killing by the hok/sok system of plasmid R1. Sok antisense RNA regulates hok gene expression indirectly through the overlapping mok gene. J Mol Biol. 223: 41-54.

Van Melderen, L., Bernard, P., and Couturier, M. (1994) Lon-dependent proteolysis of CcdA is the key control for activation of CcdB in plasmid-free segregant bacteria. Mol. Microbiol. 11, 1151-1157.

Wang, X., Lord, D.M., Cheng, H.Y., Osbourne, Do., Hong, S.H., Sanchez-Torres, V., Quiroga, C., Zheng, K., Herrmann, T., Peti, W., Benedik, M.J., Page, R., Wood T.K. (2012) A new type V toxin-antitoxin system where mRNA for toxin GhoT is cleaved by antitoxin GhoS. Nat. Chem. Biol. 8: 855-861.

Wang, X., Lord, D.M., Hong, S.H., Peti, W., Benedik, M.J., Page, R., Wood, T.K. (2013) Type II toxin/antitoxin MqsR/MqsA controls type V toxin/antitoxin GhoT/GhoS. Environ. Microbiol. 15: 1734-1744.

Whitaker, W.B., Richards, G.P., Boyd, E.F. (2014) Loss of sigma factor RpoN increases intestinal colonization of *Vibrio parahaemolyticus* in an adult mouse model, Infect Immun. 82: 544-556.

Wong, H.C., Wang, P. (2004) Induction of viable but nonculturable state in Vibrio parahaemolyticus and its susceptibility to environmental stresses. J. Appl. Microbiol. 96: 359-366.

Xu, H., Roberts, N., Singleton, F.L., Attwell, R.W., Grimes, D.J., Colwell, R.R. (1982) Survival and viability of nonculturable Escherichia coli and Vibrio cholerae in the estuarine and marine environment, Microb. Ecol. 8: 313-323.

Xu, SY. (2015) Sequence-specific DNA nicking endonucleases. BioMol Concepts 6: 253-267.

Yamaichi, Y.M., Fogel, A., Waldor, M. K. (2007) *par* genes and the pathology of chromosome loss in *Vibrio cholera*, Proc. Natl. Acad. Sci. USA. 104**:** 630-635.

Yuan, J., Sterckx, Y., Mitchenall, L.A., Maxwell, A., Loris, R., Waldor, W.M. (2010) Vibrio cholerae ParE2 poisons DNA gyrase via a mechanism distinct from other gyrase inhibitors, J. Biol. Chem. 285: 40397-40408.

Zhang, J., Ito, H., Hino, M., Kimura, M. (2017) A RelE/ParE superfamily toxin in Vibrio parahaemolyticus has DNA nicking endonuclease activity. Biochem Biophys Res Commun. 489: 29-34.

Acknowledgements

I deeply express my sincere gratitude to my research supervisor, Professor Emeritus **Makoto Kimura**, for his patience, encouragement, and constant guidance throughout this project.

I am very much obligated to Professor **Yoshimitsu Kakuta** (Lab. of Structural Biology and Biophysics, Kyushu University), for kindly help and suggestion during my research.

I feel very honored to have Associate professors **Yoshinori Katakura** (Lab. of Cellular Regulation Technology, Kyushu University) and **Kosuke Tashiro** (Lab. of Molecular Gene Technics, Kyushu university) reviewed my doctoral thesis.

My appreciated to **Professor Makoto Ito and Associate Professor Nozomu Okino** (Lab of Marin Resource Chemistry, Kyushu University) for the remarkable help and advices in the experiment of gene-knock-out.

I wish to express my gratitude to Professor **Tsutomu Katayama** and **Saki Taniguchi** (Graduate School of Pharmaceutical Sciences, Kyushu University) for their valuable discussion and help in fluorescence microscopy and flow cytometry.

I am also grateful to Professor **Yoshizumi Ishino** (Lab of Protein Chemistry and Engineering, Kyushu University) for his kindly discussion and help.

I express my thanks to Assistant Professor **Takashi Nakashima** (Lab of Biochemistry, Kyushu University) for help in my experiment.

I offer my thanks to Ph D. Toshifumi Ueda (Kyushu University) for his valuable discussion and help in my experiment.

I also thank all the members in my research group, Dr. Madoka Hino, Mr. Tomonori Natsume, Mr. Hironori Ito, Mr. Yuki Hirashima and Mr. Yuto Horikawa, for challenging a new field.

I am extremely thankful to all members in the laboratory of Biochemistry.

I am grateful for the financial support from CSC (Chinese Scholarship Council).

I appreciate so much for those encouragement and help from my Mom and Brother and my lovely friends.